POLITECNICO DI TORINO

Corso di Laurea Magistrale
in Ingegneria Energetica e Nucleare

Tesi di Laurea Magistrale

Optimization algorithms applied to e-bus charging stations in Toronto

Relatore

Prof. Maurizio Repetto

Co-relatore

Prof. Hossam Gaber (UOIT, Ontario, Canada)

Candidato

Francesco Pino

Settembre 2018

SUMMARY

1) INTRODUCTION

Energy requirement is growing last years due to world increasing population and economy, and this is one of the most important problems of the new millennium. The challenge that our generation need to consider starts from the fact that traditional fuels are typically not renewable and additional and alternative energy sources only can prevent a world energy crisis.

Second important problem is that, according to a commonly accepted scientific theory, burning fossil fuels are causing temperatures to rise in the earth's atmosphere in a phenomenon called global warming. Its effects, together with those of pollution, are revealing year after year as predicted and are getting more and more dangerous [1].

The use of alternative fuels is an essential step towards enhancing the quality of our environment and to contain also mentioned problems. They considerably decrease harmful exhaust emissions (such as carbon dioxide, carbon monoxide, particulate matter and sulfur dioxide) as well as ozone-producing emissions [2].

In this thesis there is the work of a study from UOIT (Canada) search lab where I was involved. Work face up to introduced problems in the transportation area. This sector is actually an important slice of global energy consumption (20%) and it is dominated for 92% by two fuels: motor gasoline and diesel. Introduction and improvement of electric vehicles in an important act to increase the percentage of alternative fuels and stand up to traditional source crisis [3].

Employment of electric vehicle in public and private use is for sure the correct way for the future transportation to tackle problems in this sector [4][5]: however, this switch lead to various topics that need to be faced and solved.

The aim of this thesis is the optimization in two important fields of public transportation. Application case is the city of Toronto and the future scenario studied is the public bus network switched from traditional fuels to electric one. Optimization needs to be the core business of the growth of electric vehicles since waste energy means directly waste money and it in future scenarios needs to be avoided. Alternative fuels are not directly exploited and are not always available in the scenario of public transportation but can be storage and then used in the time. This explain why to waste energy is not recommended.

First half of the thesis deal with some features about electric bus and then studies the optimal number and the placement of the fast charging stations in an urban area. Constraint of this work is the distance between bus end stop and relative station in order to waste as low as possible time and energy to cover

the distance. Optimization algorithms involved in the work are descent gradient (DG) and genetic (GA) that are applied separately and combined to find the best solution using MATLAB. Case study of Toronto area prints a real case application with numerical results.

Second application of optimization algorithms is the internal design of the fast charging station. They are equipped with and energy storage to cover the peak and to have energy available even when renewable sources are not directly active. Actual best system is the flywheel storage that is described in a SIMULINK model. Optimization works in the PID control involved in the torque model of the system and its aim is to improve the performance with a higher value and a faster response. MATLAB implement another optimization algorithm called artificial immune system (AIS) that enhance the traditional work of the control.

2) OPTIMAL ALLOCATION PROCESS

Charging station infrastructure is for sure one of the important sides of electric vehicle world, and this thesis studies the optimal implementation of electrical DC Fast Charging Stations [6], that permit a battery charge time of 15 minutes, in a city bus network.
In particular, the aim is to find the optimal number of required stations and to stem the cost and the time due to the way from bus route to station to charge the battery in the case study of Toronto area.
Following work carries out equation to forecast the number of charging stations and the target equation about minimizing cost and its constraints.
Minimization of cost problem will be reduced to optimization of distance between bus routes and relative FCS; it will be solved with enhanced neural method and integrated graphically with Voronoi diagram.
Efficacy of the methods is reflected another time in the last section, where different applications shows the economic saving due to optimization siting work of bus FCS.
Work needs a first and preliminary work to obtain a background situation to reach the first aim previously introduced.
To minimize costs and consumptions through the optimal allocation we need to know various aspects of the network that is under examination. In particular, the number of bus involved and their main characteristics, that reflect in their average consumption (kWh/km), distance covered in each route and the number of charging stations placed in the area. Another important characteristic that let to place optimally the stations concerns about the frequency of the bus at the bus stop, which reflects on the waiting time of the vehicle at the charging station and that will be studied in one of the next paragraphs.
Following preliminary work let us to determine target equation that needs to be studied and minimized and a complete view of charging stations and electric buses in the area.

2.1) DEMAND PREDICTION

To switch a bus network from traditional fuel to electric vehicles, first step is to forecast electricity and power demand in the planning region. The design of the FFCS structure itself equipped with an energy storage [7] is actually another great step of this work. Starting point to have the electrical demand for each route is to have data about distance traveled and energy consumption of the vehicles.
Equations (1) and (2) represents a specific view of the calculation of the energy demand where starting assumption is that buses charge the battery at the end of each route. It is a simplifying but reasonable

hypothesis basing on the energy consumption and dimension of the bus battery, as we can see in following description. Basing on different charging mode, next equations can be simply modified.
Electric demand per route for each bus is:

$$w = C_{av} \cdot d_i \tag{1}$$

Where $C_{av,i}$ is the average consumption of vehicles [kWh/km] and d the total distance of the route [km].
To forecast the total daily energy demand in the planning region the equation is extended in this way:

$$W = \sum_{i=1}^{N} w_i \cdot n_i \tag{2}$$

Where N is the total number of bus in the area, and for each of them n is the number of charging cycles per day.

2.1.1) BUS BATTERY

An important feature that is important in this study is the energy consumption of bus battery. Since it is a developing topic, there is an introduction about modern and more reliable technologies that are actually applied to electric bus [8]. In this way it is easier to read and understand the case study that is presented in following chapter.
Actual research work on battery is leading to the increment of lithium-ion (Li-Ion) batteries, replacing the previous technology based on nickel-metal hydride (NiMH) [9].
The higher value of energy and power density is the main reason of the switch from the old solution to the other with a lighter metal. In fact, there are two of the main parameters of performance indicator of an energy battery next to lifetime, reliability and storage efficiency.
Lithium-ion batteries are currently used in electric and hybrid vehicles. There are different type of lithium batteries and now the most favorable for use in electric buses are analyzed.
The charging and discharging modes are associated with the transfer of lithium ions through the electrolyte.
Li-ion cells are characterized by their cathode material because the anode is usually based on carbon (graphite or hard-carbon), except LTO cells that are actually the best solution for bus batteries due to many reasons. Main one is the good job at high temperature.

In this family, basic materials used on the cathode side are lithium cobalt oxide (LCO), lithium nickel oxide (LNO), spinel lithium manganese oxide (LMO) and lithium iron phosphate (LFP). It is additionally useful to find lithium nickel cobalt aluminum oxide (NCA) and especially lithium nickel manganese cobalt oxide (NMC) that are two mix of the first three types of cells.
In particular, for electric bus charging stations, test for lifetime and fast charging operations are performed with the application of a suitable load profile [11].

I. LTO batteries

In LTO batteries (Lithium-titanite) the anode is made of titanium oxide ($Li_4Ti_5O_{12}$). They can operate in temperatures between -46°C (charging and discharging) and 70°C, more than other batteries and can be charged with high voltage.
Current studies show that they have a capacitance of 90 Wh/kg and 250 Wh/dm^3.
The properties of this kind of batteries is ideal for the electric buses that need to charge frequently and with rapid times because tests show that after thousands of cycles of full charging their capacity decrease just of some percentage points (fig. 1).

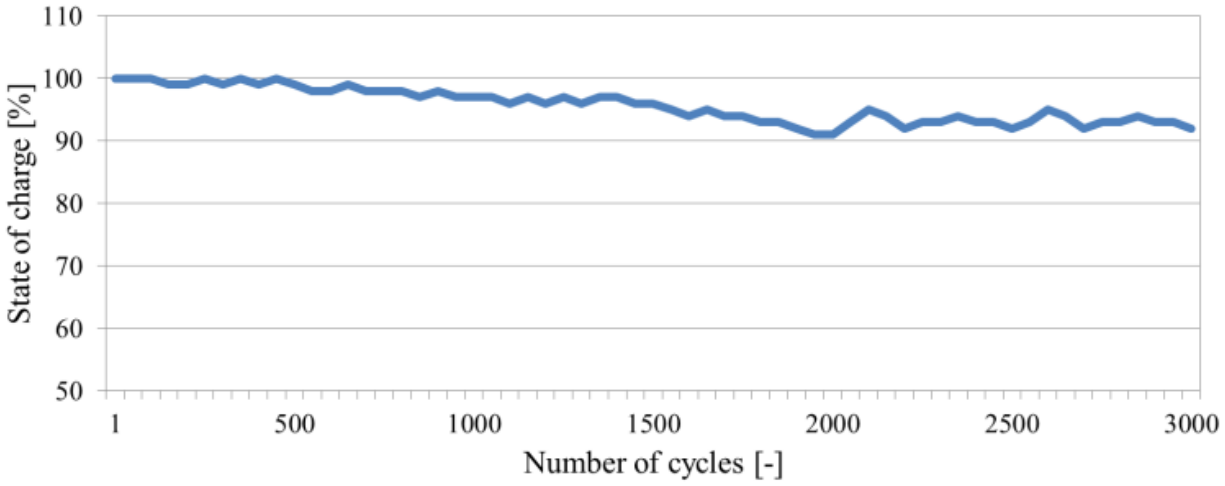

Figure 1- State of charge during life (LTO)

II. LFP batteries

LFP batteries (Lithium ferro phosphate) are characterized by the cathode made of lithium compound, iron, phosphorus and oxygen (LiFePO4).
Working temperature range between 0 and 60°C, and the energy density reaches over 120 Wh/kg, which is a high and desirable value.

To compare with previous battery, LFP after 2000 full cycles reduces its capacity to 80% of original one (fig. 2).

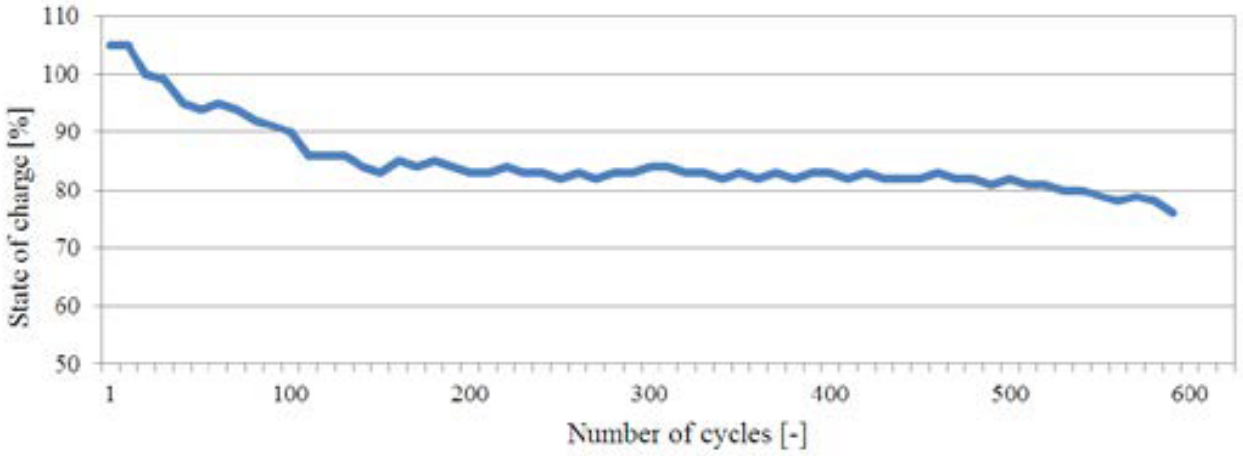

Figure 2- State of charge during life (LFP)

LFP batteries, due to higher specific energy than LTO batteries, can be ideally used in electric buses that need to cover an extended route with only one charge. In the case study they are actually used for the night buses that haven't time to stop after each night route.

2.1.2) e-BUS CHARGING SOLUTIONS

The charging infrastructure and charging modes follow requirements and strategy of the bus network. There is a direct connection between charging time, power and battery size. Extreme cases are very fast charging, that is more frequently and that requires high power from grid and a smaller battery, while on the other side there is a less frequent charge, with lower power need and with larger battery. First case is when electric bus charge every stop, while second example is depot overnight charge.

From all of these features, the most important are that in one case strategy requires an expensive battery while, on the other hand, it requires expensive chargers due to high power. In addition it must be considered that large batteries will reduce passenger capacity.

Between these two cases, there are other possibilities to charge: for example only at end stations or a few stations along the route. In this way a good strategy can exploit both pros and reduce cons.

Stop only at terminal station is actually the best compromise, considering energetic and economic sides.

Figure 3- Solutions field

2.2) NUMBER OF CHARGING STATIONS

One of the most important preliminary study is the determination of the number of charging station to place in the city area. Many studies on electrical bus networks put the station at each stop or at the terminal stop of the track or at the depot.

The aim of this work is to minimize cost for infrastructure and optimize collection of renewable energy with an energy storage. In order to reach these goals, this section will calculate the number of charging stations that a case study needs to put in its work. The idea is to have various common areas for the buses that need to charge their battery between one route and the next one. Buses usually have fixed track and thanks to actual supercapacitors they need only 15-20 minutes to charge the battery for an average city route. In this way they can respect their time schedule charging their battery in a near common area. This will reflect on a first cost saving due to the reduction of number of charging infrastructures and additionally charging other electric vehicles, like car, can use stations if service is available, since following calculation is conservative.

Every case study will be different from the other and in this way equation (3) is adaptable for every situation. Since all bus in the network has to follow a time schedule, the number of charging station is calculated in order to ensure the correct operation of the buses in the worst (and almost impossible) scenario, that is when all the buses of the city are going to charge their battery contemporary.

$$\mathrm{CS} = \frac{\#\ \text{charging bus}}{\#\frac{\text{substations}}{\text{stations}} \cdot \#\ \text{waiting slot}} \tag{3}$$

Numerator of equation (3) is the maximum number of vehicles that could be at the station to charge. Depending on the future or real schedule, this is the described worst situation previously mentioned. In following case study all bus fleet is included in the calculation to be conservative for future changes in the network too.

Denominator of the ratio is influenced by two factors: first is the ratio between the total number of substations and charging stations that represents the average number of substations per station and the second is the charging time. Last factor is reflected in the equation through the number of charge slots that each bus can wait before charging in order to respect its schedule.

2.3) DETERMINATION OF TARGET EQUATION

After the identification of the number of charging stations next step is the initial positioning in the area. Usually they can be initially distributed in a regular way in order to have a certain uniformity even if they will be moved after optimization. Actually, initial position can influence final one, jointly with other constraints that user imposes. Basing on each different situation starting position can be clearly different from one case study to the other.

In particular, the objective function to be minimized in this situation is the total cost when each bus goes from its terminal stop to the relative charging station before starting new trip.

This factor is influenced by the consumption of the vehicle (kWh/km), the cost of the electric energy ($/kWh) and the total distance to go to charge the battery (km).

$$C = \sum_{j=1}^{N} C_{av,j} \cdot G \cdot [(x_j - a_j)^2 + (y_j - b_j)^2]^{\frac{1}{2}} \tag{4}$$

Where N is the number of the bus in the studied network, $C_{av,j}$ is the energy consumption of each bus vehicle (kWh/km), G is the cost of energy ($/kWh), x_j and y_j are the coordinate of bus stop, while a_j and b_j are the coordinate of the charging station of the relative bus.

In this paper, the work focuses on the last part of the equation, which is the total distance “d” between each bus terminal and its charging station:

$$F(x,y) = d = \sum_{j=1}^{N} [(x_j - a_j)^2 + (y_j - b_j)^2]^{1/2} \tag{5}$$

In fact, leaving C_{av} and G fixed, minimizing this factor leads to a minimization of the total cost function. To make d get the minimum value means to obtain the optimal coordinate of FCSs (a,b) and to do this

Enhanced Heuristic Gradient Descent method is applied and results are shown and discussed in next sections.

Constraints to implement in the methods are geographical and mathematical:

1) Coordinates of FCSs have to be within the boundaries of the planning area;
2) Impose a minimum distance between one FCS and the nearest, based on the needs and properties of the city.
3) Impose a minimum threshold between successive results of the MATLAB cycles.

In this way initial coordinate points will move to final and optimal ones respecting constraints just mentioned.

3) OPTIMIZATION ALGORITHM

Since the goal of this first part of the thesis is to optimize a certain function previously described, in this chapter two of the best optimization methods are applied. In particular, bus network needs to minimize daily distance (and cost) to go to charge electric battery between two successive roads.

3.1) DESCENT GRADIENT METHOD

Descent Gradient is a first-order iterative optimization algorithm invented by Cauchy in 1847. Its concept is very easy but at the same time it is one of the most robust tools for optimization problem [15]. In the case study of this analysis, final aim is to find the minimum of the described function to place optimally the stations [16].

At each step of the algorithm, the gradient of the error function is calculated and the free parameter of the system (in this case the coordinates) is updated to make a small step in the opposite direction to the gradient. Next, the gradient is recalculated for the new solution, and this step is repeated until a maximum number of iterations is reached or the size of the gradient falls beneath a threshold.

Gradient descent is based on the observation that if the multivariable F(x) is defined and differentiable in a neighborhood of a point "a", then F(x) decreases fastest if one goes from "a" in the direction of the negative gradient of F at x, $-\nabla F(x)$. With this observation, one starts with guess x_0 (initial coordinates) for a local minimum of F, and considers the sequence $x_0, x_1, x_2\ldots$ such that:

$$x_{n+1} = x_n - \gamma_n \nabla F(x_n), n \geq 0 \quad (6)$$

Where γ_n is the step size and $\nabla F(x_n)$ is the gradient of the function:

$$\nabla F(x_n) = \left[\frac{\delta F}{\delta x}, \frac{\delta F}{\delta y}\right] \tag{7}$$

Finally, note that the value of the step size γ can be a constant or an adjustable value. Second one is a better solution and it change at every iteration; in particular, local minimum is guaranteed with following choice:

$$\gamma_n = \frac{(x_n - x_{n-1})^T [\nabla F(x_n) - \nabla F(x_{n-1})]}{\|\nabla F(x_n) - \nabla F(x_{n-1})\|^2} \tag{8}$$

This algorithm will lead to have:

$$F(x_0) \geq F(x_1) \geq F(x_2) \ldots \tag{9}$$

So actually the sequence (x_n) converges to the desired local minimum.

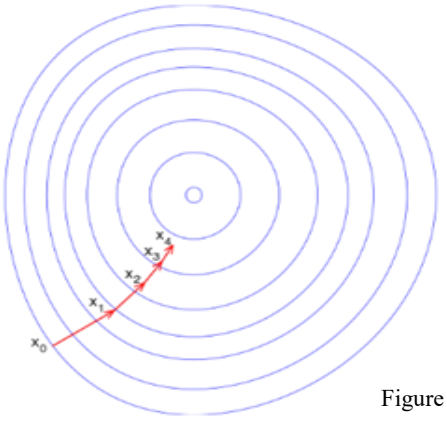

Figure 4-Illustration of gradient descent solutions.

Descent gradient method works both with linear and non-linear equations, and in infinite-spaces dimension [17].

The application of the algorithm will stop when some conditions are reached. In the case study of this thesis, during optimization algorithm, some boundary conditions need to be ensured are.

- Charging stations clearly need to stay in the border of the town area;
- Between two successive cycles, the change of the fitness value with respect to previous is less than a threshold;
- Minimum distance value between two stations.

It is assumed that FCS fast charging stations are placed in the area and their initial positions can be mathematically defined. The region can be represented in a Voronoi diagram [18], which initial vertices are initial FCSs points and in the end each subregion will contain a charging station that is the nearest for all bus within.

a) Generate initial FCSs points: planning area is divided equally in a grid basing on the CS value and the points at the intersection of the lines are starting coordinates;
b) Position in the planning area the points related to the bus terminal;
c) Calculate total distance from each bus terminal and its nearest FCS and the total cost with the target equation;
d) Application of descent gradient method in order to minimize total distance, which results are new coordinates of stations;
e) Move locations to the new and best positions;
f) Recalculate new total distance and consequently new total cost and check if one of the following conditions is reached: if "Yes", results are optimal coordinates of FCS, if "No" come back to step d) and repeat cycle until constraints end optimization work.

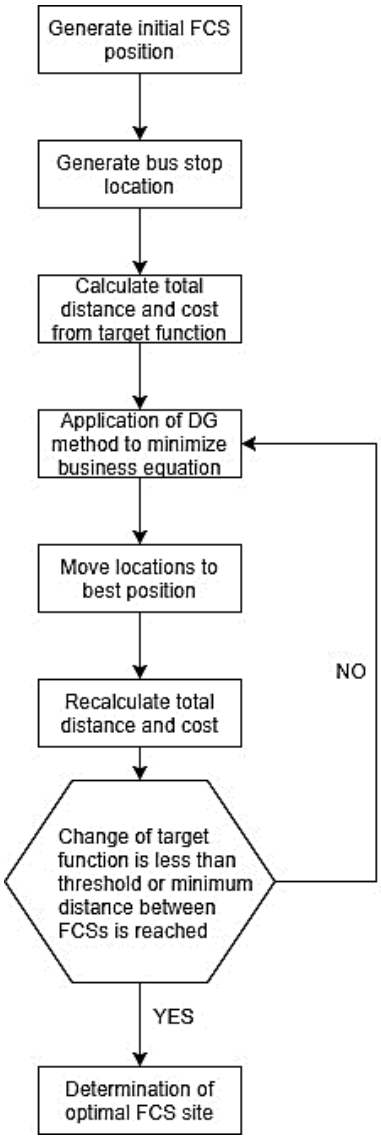

Figure 5- Flow of DG method

3.2) HEURISTIC GENETIC ALGORITHM

Heuristic methods are used mostly with non-linear equations, when problem solutions are heavy, and they indeed need a great computational cost due to numerous numbers of iterations to reach optimal solution.

HGA will apply theory of evolution by utilization of evolutionary process to find the optimal solution of a problem [19]. A member of a population generation of the GA is represented by its chromosome. It follows and try to simulate the “survival of the fittest” mechanism of selection studied by Darwin in his theory, where it means that only fittest phenotype can survive to a test and enhance future generations.

In particular, its skill comes from the ability to pull out information from previous generation in order to increase performance of future one. New set of artificial chromosomes is created using bits and pieces of the fittest of the old ones through the operation of reproduction, crossover and mutation.
Due to the probabilistic process, even the weakest part of the population has a chance of reproduction and simultaneously fittest members may not be preserved in next generations.
In order to overcome this problem, solution is to track the fraction of fittest individuals as elite and copy their best-fit string to next generation without crossover and mutation processes. It begins with a set of solutions represented by population and, at each step, it selects individuals from the current population to be optimized source and uses them to produce the new transferred optimized solution for the next epochs [21] [23].
Crossover and mutation are the functions that create the offsprings that will form the next generation. First uses a digital analogue mechanism of sexual reproduction, randomly choosing substrings from two parents from their chromosomes and splicing them together at a crossover point.

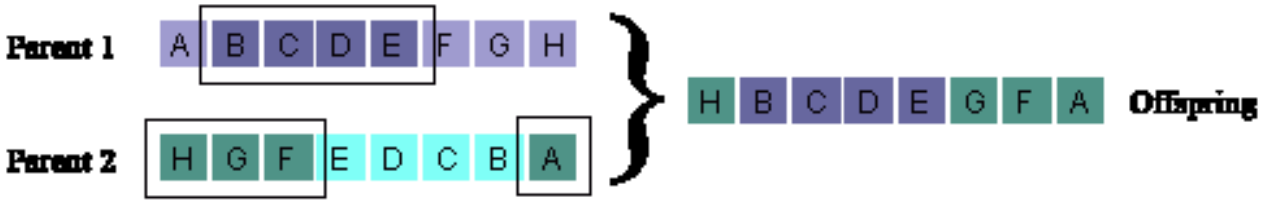

Figure 6 Sample offspring created by splicing genes of selected parents at a crossover point.

Mutation function performs some offspring of the next generation by mutating the genome of individual parents. Its aim is to keep diversity among members of population and avoid an early convergence towards a local maximum.

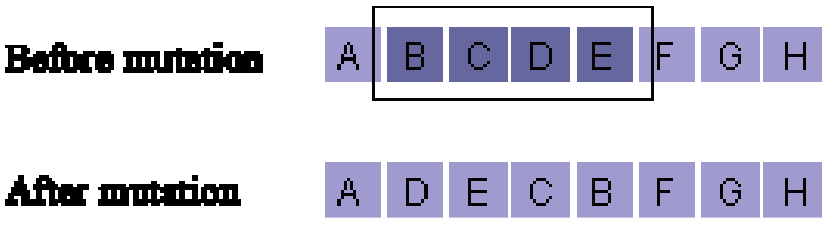

Figure 7 Sample offspring created by mutating genes of a selected parent

By objective process, the fitness of actual member is determined using the function F(x). F(x) is the fitness function previously described that need to be optimized. In this way each member has a weight that reflects on its influence on the next generation.

The population on-line performance P(x) is defined as:

$$P(x) = \frac{1}{P}\sum_{p=1}^{N} F_t^x(p) \quad \text{n=0,1,.....,T-1} \tag{11}$$

HGA decline the worse solution patterns, and keep the highest probability ones, to check and confirm the diversity capability, d_{ij} which is the distance of variables between two solutions X(i) and X(j) is calculated:

$$d_{ij} = \sqrt{\sum_{K=1}^{S}\left(\frac{X_k^{(i)} - X_k^{(j)}}{X_k^{max} - X_k^{min}}\right)^2} \tag{12}$$

The fitness values are then used to prioritize by definition of selection probability to select the best patterns moved to the new solution cursor.

$$\text{Probability } i = \frac{1}{\|P\|}\left(2-\alpha+(2\alpha-1)\frac{i-1}{\|P\|-1}\right) \tag{13}$$

α represents selection bias as higher values lead to direct the cursor to select only the well individuals with probability of $\frac{\alpha}{\|P\|}$; while worst individuals have probability of $\frac{2-\alpha}{\|P\|}$.

The convergence of solution cursor is tested by:

$$E(N_G) = 1.4\,N\,(0.5\ln(z)+1) \tag{14}$$

This is repeated until some stop criterions are satisfied.

Now various steps are specified and it will be clear how to apply it in the case of the minimization cost studied in this paper. How it is reasonable, FCSs coordinates represent the population in this work.

a) Generate population of n chromosomes, positioning the stations in desired starting locations (in the grid as previously specified).
b) Implementation of the fitness function f(x) and application of it to each chromosome in the population.
c) Generation of new population through crossover and mutation from parents that are selected because have a fitter solution to the problem. In this way problem converges to optimization.

d) Run the algorithm with the new generation and control if the algorithm reaches one of the cycle constraints:

- Minimum threshold between the two solutions.
- Minimum distance between electrical DC fast charging stations.
- Maximum number of generations.

If *Yes* the optimal solution is that of the current generation, otherwise come back to step b) and perform another cycle.

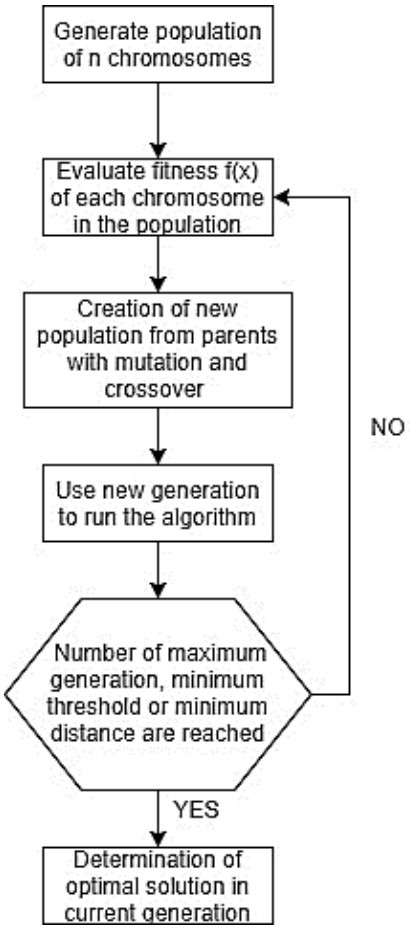

Figure 8- Flow of HGA

3.3) VORONOI DIAGRAM

In this section there is the description of the Voronoi diagram, that consist in an interesting domain discretization. In particular, the Voronoi algorithm starts with a predefined set of points called seeds and

will divide space into Voronoi cells [10]. Each cell has the property that all the inside points are closer to a specific seed from the set with respect to any others.

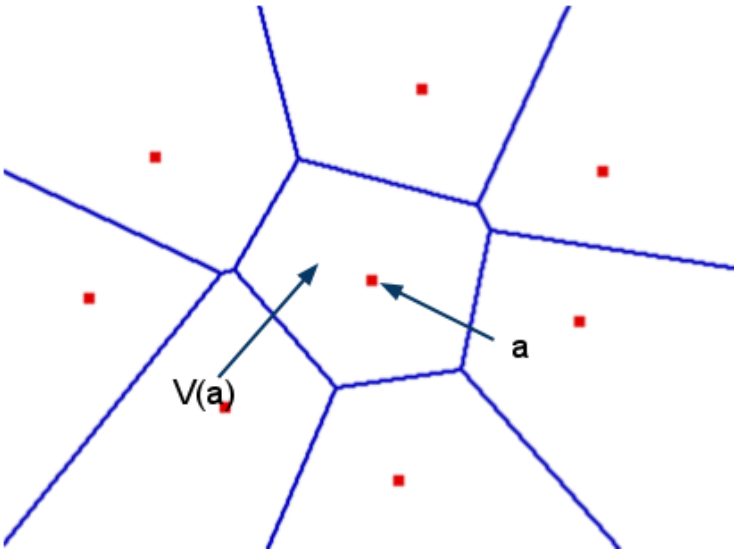

Figure 9- Voronoi diagram in 2D case

Mathematically speaking a Voronoi cell is defined as:

$$VR_k = \{d(x, P_k) \leq d\big(x, P_j\big)\ for\ all\ j \neq k\} \tag{15}$$

Where the predefined set of points P is composed of *K* elements in a metric space S. From previous equation Voronoi region *k* is composed from those points whose distance from seed *k* is lower than the distance from all the other *j* seeds, with *j≠k* [12].

A step by step definition of the Voronoi representation is assessed for the simplest case of the 2D Euclidean plane.

Institute a set P of n ≥ 3 point sites (seeds) *p, q, r,..* in the plane and define distance between two generic points a (a1, a2) and b (b1, b2):

$$d(a, b) = \sqrt{(a_1 - b_1)^2 - (a_2 - b_2)^2} \tag{16}$$

For p and q ϵ P is $B(p,q) = \{x|d(p,x) = d(q,x)\}$ the bisector line. In particular B is perpendicular to the line that connect p to q and creates two half plane. Mathematical literature defines $D(p,q) = \{x|d(p,x) < d(q,x)\}$ the half-plane containing p and *D(q, p)* the ones containing q.

Now the Voronoi region of p with respect to S is defined as:

$$VR(p,S) = \bigcap_{q\epsilon S, q\neq p} D(p,q) \tag{17}$$

Finally, following equation determinates the definition of the Voronoi diagram of set of points S:

$$V(S) = \bigcup_{p,q\epsilon S, q\neq p} \overline{VR(p,S)} \bigcap \overline{VR(q,S)} \tag{18}$$

In the Voronoi diagram the Voronoi edge is a common boundary of two cells, while Voronoi vertices are equidistant from 3 different seeds.

Last case is useful for the application of this thesis, but a n^{th}-order Voronoi diagram is always possible [13].

Each level will starts with the $(n-1)^{th}$-order diagram and then replacing each cell of that order with a successive Voronoi diagram [14].

4) CASE STUDY AND NUMERICAL RESULTS

4.1) PRESENTATION OF CASE STUDY

Previous paragraphs are useful to introduce practical work of calculation of the fast charging station number and the optimal place in an urban area. All theoretical equations are applied to the case study of Toronto and numerical results will demonstrate goodness of optimization algorithms.

Toronto has a population of more than 2'700'000 habitants and its actual area is of 630 km^2. City has already an important bus network and the applied work owns the idea to leave it as it is, but switching simply them from traditional motion to electricity. Various companies (mainly TTC) manage a total amount of 180 different routes in the planning area, with an average of 10 bus per route for a total length of 7000 km distributed in the city.

Figure 10- Historical photo

In table 1 there are details about bus consumption and routes distribution.

Parameter	Day bus	Night bus
Type of battery	LTO	LFP
Bus number	1530	270
C_{av} [kWh/km]	1.6	1.6
Weekly working hour	5:30 – 1:30	1:30 – 5:30
Charging time	15 minutes	4 h
Routes average length [km]	39	39
Trip number per day	7	2
Waiting time between two trips [h]	1	0

Table 1- Toronto route parameters

Public transport has two different schedules for daily and nightly routes. During the day there are more bus network that cover all the city more frequently, while during the night number of bus involved are less (one over six) and cover only main city routes.

Figure 11- Toronto daily bus map

Figure 12- Toronto night bus map

Previous figure represents the area of Toronto and solid red and blue points are the end stops of each bus or streetcar involved in the total network.

According to (1) and (2), the electric consumption per bus is calculated and is w=441 kWh for a work day and 125 kWh during the night trips.

Since morning motion is more frequently and involves more bus vehicles, it is expected a fast charging of 15 minutes at the end of each route. They have one hour to go to charge to the nearest station before starting new trip.

During the night the number of complete route per each bus is only 2 and then they will be charged during the day with a slower charge. This will reflect on a different kind of battery used for the vehicles. Actually LFP battery is a good option for night transport, since the bus can work 4 hours continuously, while during the day LTO is the solution for fast charging at the end of each route.

Starting from tabled parameters, application of equation (3) leads to a 26 required FCSs in the city area. After this network overview, the work proceeds with the application of genetic algorithm and descent gradient optimizations. Then a heuristic method (EHDG) is explored to optimally place the FCSs, with graphical integration of Voronoi diagram representing the area of Toronto.

4.2) APPLICATION OF OPTIMIZATION ALGORITHM

To have a certain regularity in the city starting points are the vertex of the grid that divide equally the area covered by the bus network. First step of the work is the application of previous methods (descent gradient and heuristic genetic algorithm) separately and then there will be the implementation of enhanced heuristic descent gradient, with a particular prominence to its optimization results.

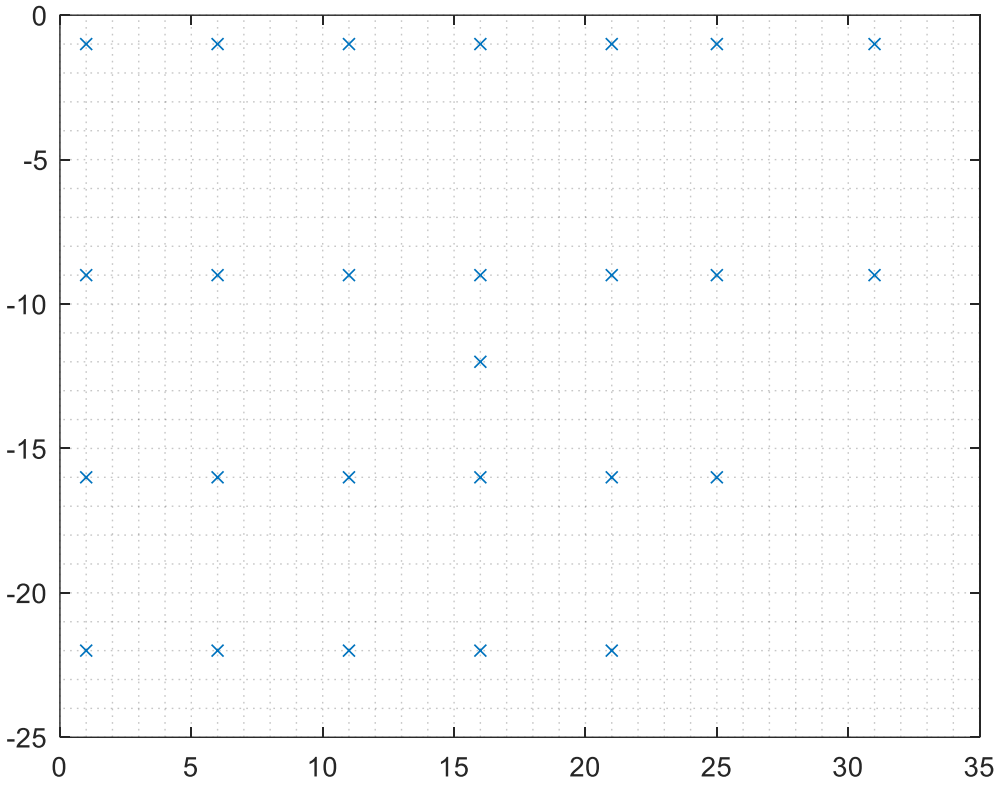

Figure 13- Starting layout of grid

4.2.1) DESCENT GRADIENT METHOD

In the application of DG, each bus stop is linked to the nearest FCS and then optimization process starts until constraints conditions are reached. Before the final result, the graph below points out how the work optimize position of stations and in particular it is clear that total distance between each bus stop and its nearest FCS decreases until the optimal value.

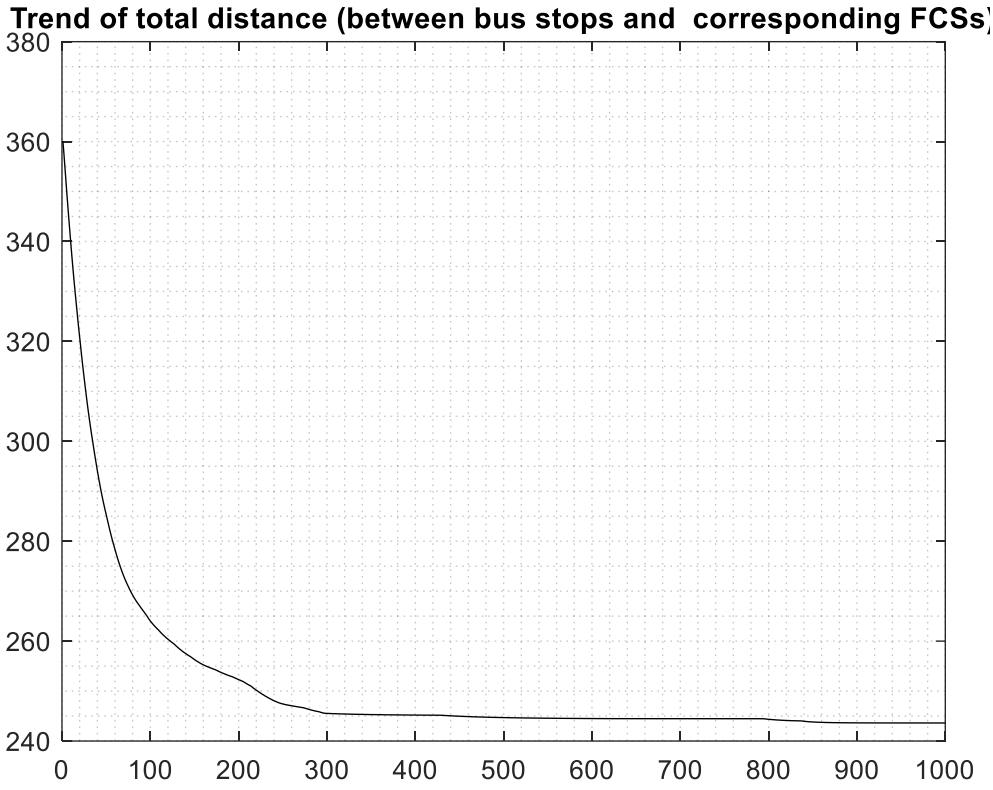

Figure 14- Trend of total distance with DG [km]

Fig. 14 shows how the value of training function optimally goes through a minimal value during the application of optimization algorithm. Since its value represents the total distance value from each bus stop and its relative and nearest FCS, the decrement from 360 km to 243 km reflects on a significant improvement of FCS siting during the simulation.

In fig. 15 red cross are the terminal bus stop previously showed in the real map of the city, while black dots are final positions of the FCSs.

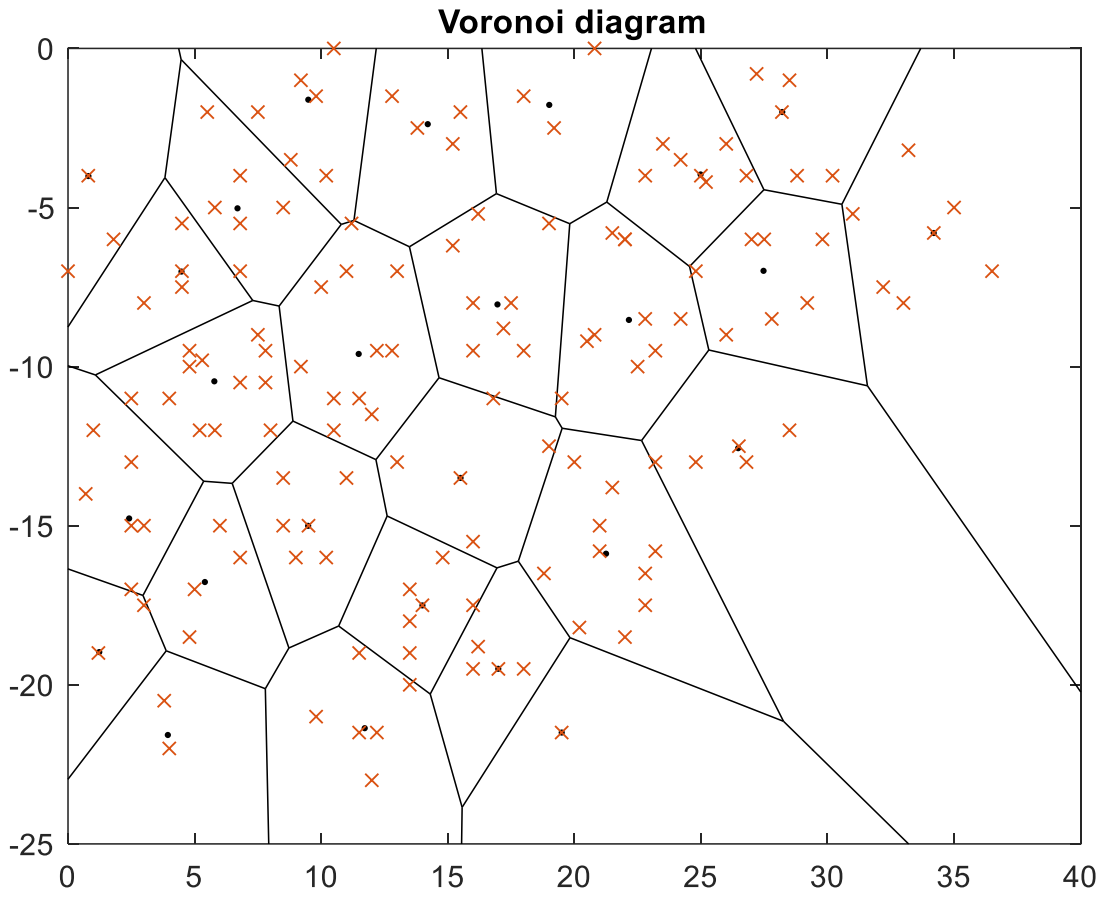

Figure 15- Final positions of FFCS

Following text shows how to implement main part of the described descent gradient method in a MATLAB code.

It is clear how the positions move towards best positions (Fig.15) and optimally in the bus stop cobweb, until constraints are reached.

Box #1 shows the constraints that will restrict the run of the algorithm. A minimum distance between the stations and a maximum number of cycles are applied in this work. First value is suggested from a practical situation in the town to avoid having two FCSs near their self and to cover in a better way the area. Second constraint value comes from the evaluation of similar simulation that evidence that in 1000 cycles work is already optimized or almost done.

Box #2 contains calculation of partial differential equation, that are useful for the gradient formulation.

$$\nabla F(x_n) = \left[\frac{\delta F}{\delta x}, \frac{\delta F}{\delta y}\right] = \{\dots\} \tag{19}$$

$\frac{\delta F}{\delta x} = \frac{x-a}{\sqrt{(x-a)^2+(y-b)^2}}$	$\frac{\delta F}{\delta y} = \frac{y-b}{\sqrt{(x-a)^2+(y-b)^2}}$

Table 2- Partial differential equations

Then there is the evaluation of the value of the training function d for current cycle for each bus stop to its nearest FCS.

Box #3 shows the application of the core of the descent gradient method. Successive x_n (coordinates) come from:

$$x_{n+1} = x_n - \gamma_n \nabla \mathrm{F}(x_n), n \geq 0 \tag{20}$$

And in this phase of the work all variables are known. This step is very important and represents a step forward the optimal position of the stations. Reduction of total distance between each bus stop terminal and relative station between two successive cycles reflects goodness of the work that walks in the correct direction.

Box #4 involves an array of distances. This tool contains in each step all distances between FCSs in order to control and respect the minimum distance. Once that this value is reached the optimization algorithm will stop.

```
while min_distance>1 && cont<1000
```
 # 1

```
%% Start of descent gradient method
   %contatore
   cont=cont+1;

   %partial derivates
   fx=zeros(1,length(x0));
   fy=zeros(1,length(x0));
   d(cont,length(a))=0;

    vett0=[x0;y0];
```
 # 2

```
    %first for cycle for each station
    for j=1:length(x0)
    %second for cycle for each bus stop
    for i=1:length(a)
    if matrix(i,j)~=0
    fx(j)=fx(j)+(x0(j)-matrix(i,j))/(sqrt(((x0(j)-matrix(i,j))^2)+((y0(j)-matrix_2 ↙
(i,j))^2)));
    fy(j)=fy(j)+(y0(j)-matrix_2(i,j))/(sqrt(((x0(j)-matrix(i,j))^2)+((y0(j)- ↙
matrix_2(i,j))^2)));

 %total distance function (for each bus stop to nearest FCS)
 d(cont,i)=d(cont,i)+sqrt((x0(j)-matrix(i,j))^2+(y0(j)-matrix_2(i,j))^2);
 end
 end
```

```
  %antigradient
  p=-[fx;fy];
   for i=1:length(p)
     if p(i)==0
          p(i)=0.01;
     end
  end
```

```
 %new stations coordinates
 vett1=vett0+alfa*p;
```
 # 3

```
  %ri-definizione
  x0=vett1(1,:);
  y0=vett1(2,:);
```
 # 4

```
 % Request of minimum distance between stations

 for k=1:length(x0)

     for t=1:length(x0)

         if k~=t
             distance(k,t)=sqrt((x0(k)-x0(t))^2+(y0(k)-y0(t))^2);
         end
         if k==t
             distance(k,t)=5;
         end

     end
 end
```

Figure 16- MATLAB code

4.2.2) HEURISTIC GENETIC ALGORITHM METHOD

Genetic algorithm starts from the same initial points of previous method and runs for about 700 generations, when minimum threshold is reached and optimization work put out final coordinates.
Trend of target function is shown in Fig. 17; while the Voronoi diagram (Fig.18) represents the areas in which bus have their final reference stations.
As Fig.17 evidences, the optimization algorithm works well through the simulation, but the final value of the target function is higher than in previous case. This leads to consider previous DG algorithm a little better than this one.

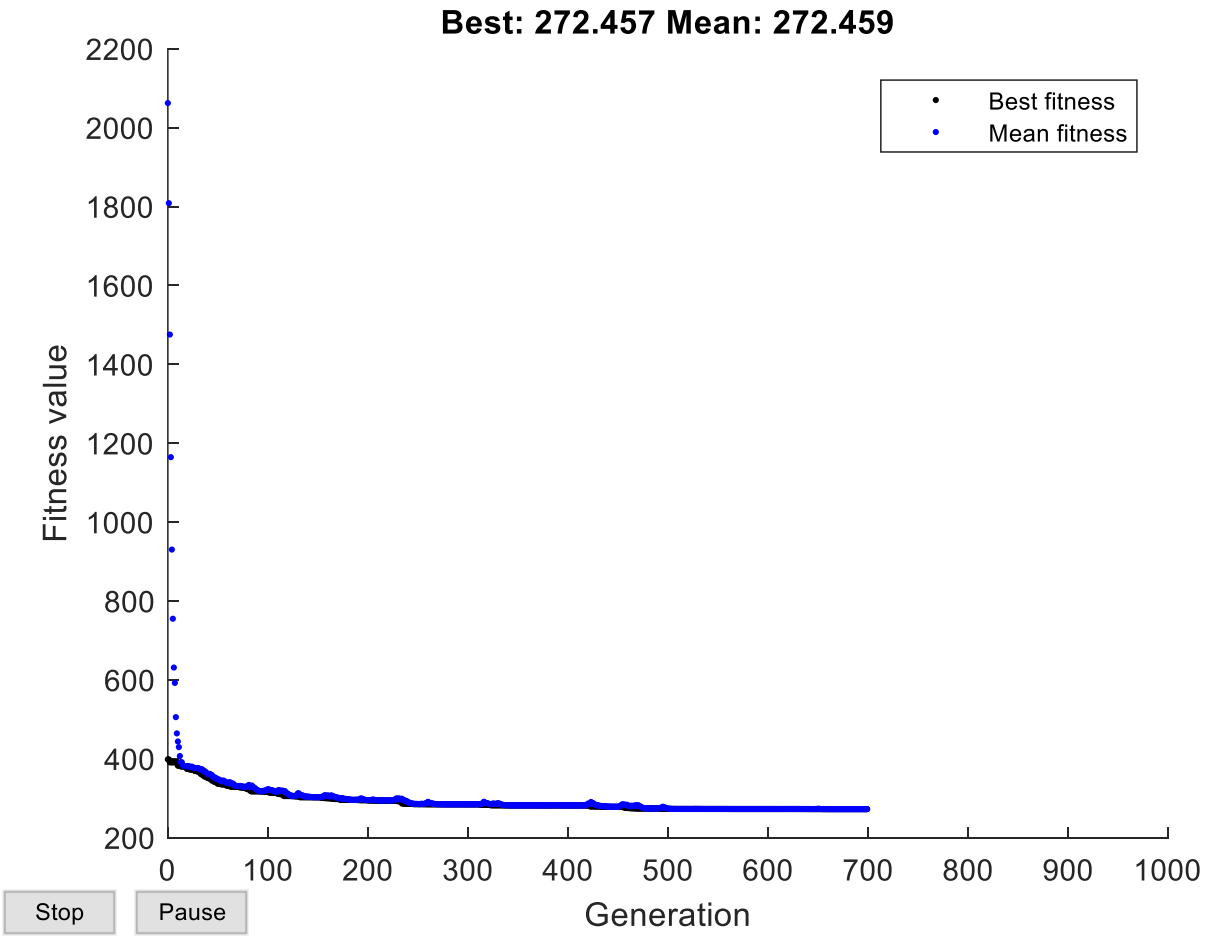

Figure 17- Trend of total distance with GA [km]

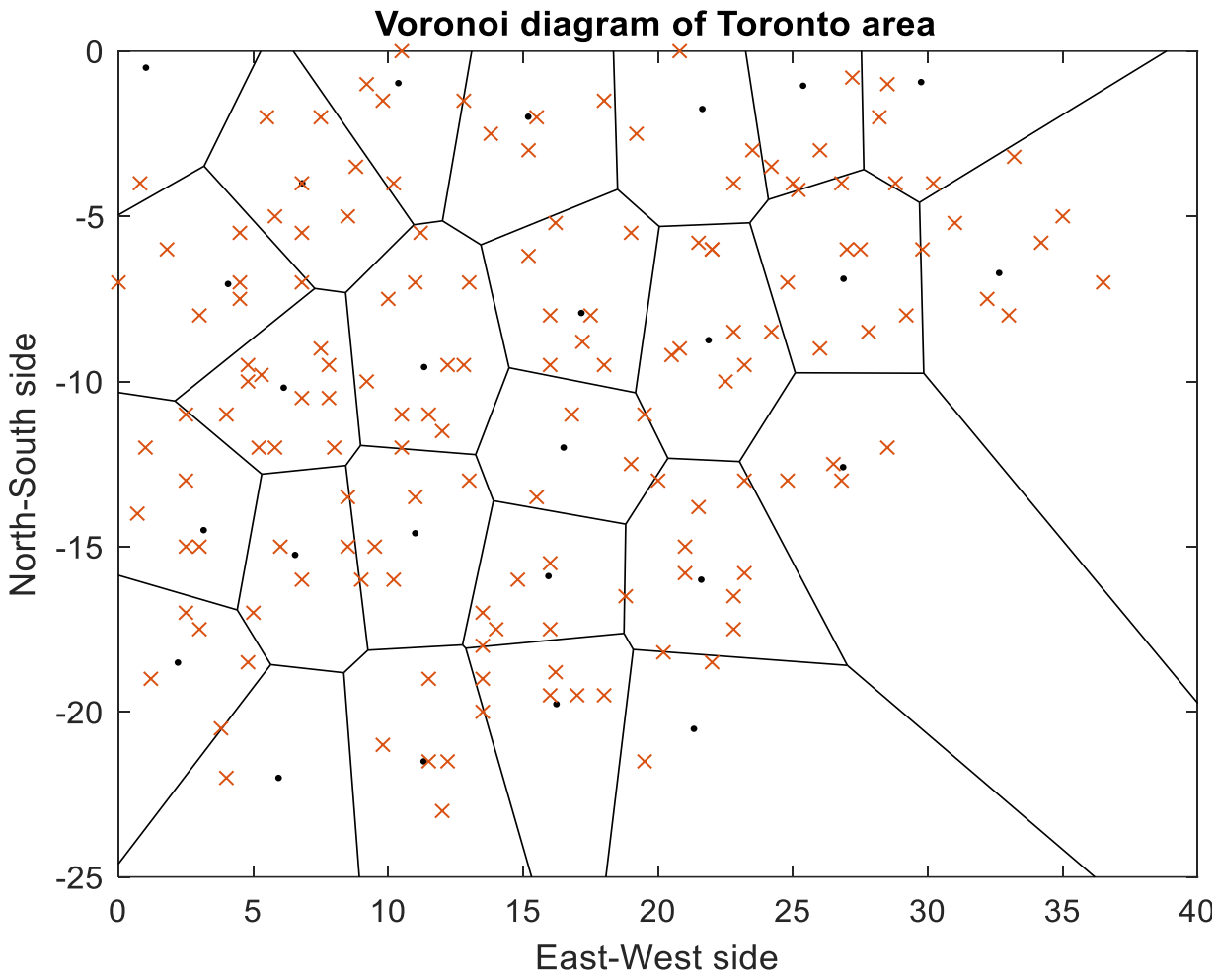

Figure 18- Final positions

The syntax used for this problem is the following:

[x, fval, exitflag, output, population, scores] = ga(ObjectiveFunction,nvars,[],[],[],[], LB, UB, [], options)

Basic ***ga*** tool finds the minimum of a function.

Input for this syntax are:

- Objective Function that is the target equation of the problem.
- Nvars represents the dimension of variables involved in the function. In current problem it represents the coordinates of the charging stations and consequently there are 52 variables (26 *x* and 26 *y* points).

- LB and UB represent lower and upper bounds for the solution variables, so that LB < X < UB. In this case they are the boundary coordinates of the Toronto area where stations are going to be placed.
- Options are values that are in addition involved in the optimization problem and that will be considered in the work.

Actual outputs represent:

- X is the solution of the problem that guarantees the minimum of the function. In this work it is clearly represented by the coordinates of the FCSs.
- Fval is the fitness function value during each cycle.
- Exitflag identifies and displays which constraints is reached for the algorithm stop.
- Output contains information on the performance of the cycles and of each generation.
- Population is the output with the final population involved in the algorithm.
- Scores is the value of the final population.

```
ObjectiveFunction = @UPFCob;
nvars = 52; % Number of variables
%in lower and upper bound there are first X values and then y values)
LB = [0 0 0 0 0 0 0 0 0 0 0 0 0 0 0 0 0 0 0 0 0 0 0 0 -24 -24 -24 -24 -24 -24 -24
UB = [33 33 33 33 33 33 33 33 33 33 33 33 33 33 33 33 33 33 33 33 33 33 33 33 33 0
ConstraintFunction = @UPFCco;
% bus stop coordinates
a=[0 0.8 0.7 1 1.2 1.8 2.5 2.5 2.5 2.5 3 3 3.8 4 4 4.5 4.5 4.5 4.8 4.8 5 5.5 5.8 5.3
b=-[7 4 14 12 19 6 11 13 15 17 8 17.5 20.5 11 22 5.5 7 7.5 9.5 18.5 17 2 5 9.8 12 12
%Starting points (first there are X values and then y values)
%X0=[0,0,0,7,14,21,28,31,33,33,28,10,16,8,5,5,5,15,22,25,22,15,13,8,3,9,-1,-12,-18,-1
%X0=[0.2577    1.3738    0.7682    6.8461   14.1358   19.8240   27.8264   31.0100   3
%grid_(same_of_dg)
X0=[1,1,1,1,6,6,6,6,11,11,11,11,16,16,16,16,21,21,21,21,25,25,25,31,31,16,-1,-9,-16,-
%%
%options about optimization
options = gaoptimset('MutationFcn',@mutationadaptfeasible, 'PopulationSize',20,
'Generations',1000);
options = gaoptimset(options,'PlotFcns',{@gaplotbestf},'Display','iter');
options = gaoptimset(options,'InitialPopulation',X0);
%%
%applications of ga
[X,FVAL,EXITFLAG,OUTPUT,POPULATION,SCORES] = gamultiobj(ObjectiveFunction,nvars,[],[
[X,FVAL,EXITFLAG,OUTPUT,POPULATION,SCORES] = ga(ObjectiveFunction,nvars,[],[],[],[],
LB,UB,[],options);
```

#1 #2 #3 #4 #5 #6

Figure 19- MATLAB code

Figure 19 and 20 show how genetic algorithm is implemented in MATLAB. In box #6 there is the code that recall the genetic algorithm as previously described.

Main function describes some general options that are applied in the algorithm. Target equation and constraints of the problems are called in two other functions: in @UPFCob in box #7 and #8, for example, there is the evaluation of the target equation for current cycle.

Box #2 contains lower and upper bound values that final coordinates must respect to stay inside the city area.

Box #4 has a row vector with initial coordinates of the stations and that are the same of the descent gradient case, in order to make a comparison of the two algorithms with the same initial and boundary conditions.

Box #5 is important because it contains the options that are subsequently applied and involved in the *ga* tool. In particular, it fixes the size (20) of the population that will work during optimization algorithm and the number of generations (1000) that will be performed before arriving at optimal solution. Other

two options represent the final plot figure and the initial population that is applied in the target function at the start of the process.

```
load matrix.mat;
load matrix_2.mat;

%x0=[ 0.2577    1.3738    0.7682    6.8461   14.1358   19.8240   27.8264   31.0100   33.7146   31.4985   27.8888
%y0=[-1.9662  -12.2569  -18.6402   -2.1676   -2.2789   -1.1243   -3.0958   -0.9900   -5.1742   -8.0933  -16.3961  -
a=[0 0.8 0.7 1 1.2 1.8 2.5 2.5 2.5 2.5 3 3 3.8 4 4 4.5 4.5 4.5 4.8 4.8 5 5.5 5.8 5.3 5.2 5.8 6.8 6.8 6.8 6.8 6.8 7
b=-[7 4 14 12 19 6 11 13 15 17 8 17.5 20.5 11 22 5.5 7 7.5 9.5 18.5 17 2 5 9.8 12 12 4 5.5 7 10.5 16 2 9 9.5 10.5
      #7
d=0;
            #8
  for j=1:length(a)

      for i=1:length(x0)
          pos=zeros(1,length(x0));
          if matrix(j,i)~=0
          pos(1,i)=1;
          d = d + pos(1)*sqrt((x0(1)-matrix(j,1))^2+(y0(1)-matrix_2(j,1))^2)+pos(2)*sqrt((x0(2)-matrix(j,2))^2+(
          end
      end
  end

  y=d;
```

Figure 20- MATLAB code

4.2.3) ENHANCED HEURISTIC DESCENT GRADIENT METHOD

Another results from optimization work is that initial positioning can influence the final position of the points. This is the starting idea for the implementation of a new technique, called *Enhanced Heuristic Descent Gradient*. Since previous algorithms are already two optimized works, new method applies the descent gradient method in series with genetic algorithm, in order to start with new coordinates that are for sure better (in terms of optimal positions) with respect to other random starting points [20] [22].
This theory is implemented and supported by results. Starting points of DG method are the same that are carried out by GA performance. After the run of the enhanced descent gradient, results of target equation are better than original algorithm.
The trend of total distance between each bus stop and its FCS during the optimization simulation are actually represented in future figures.

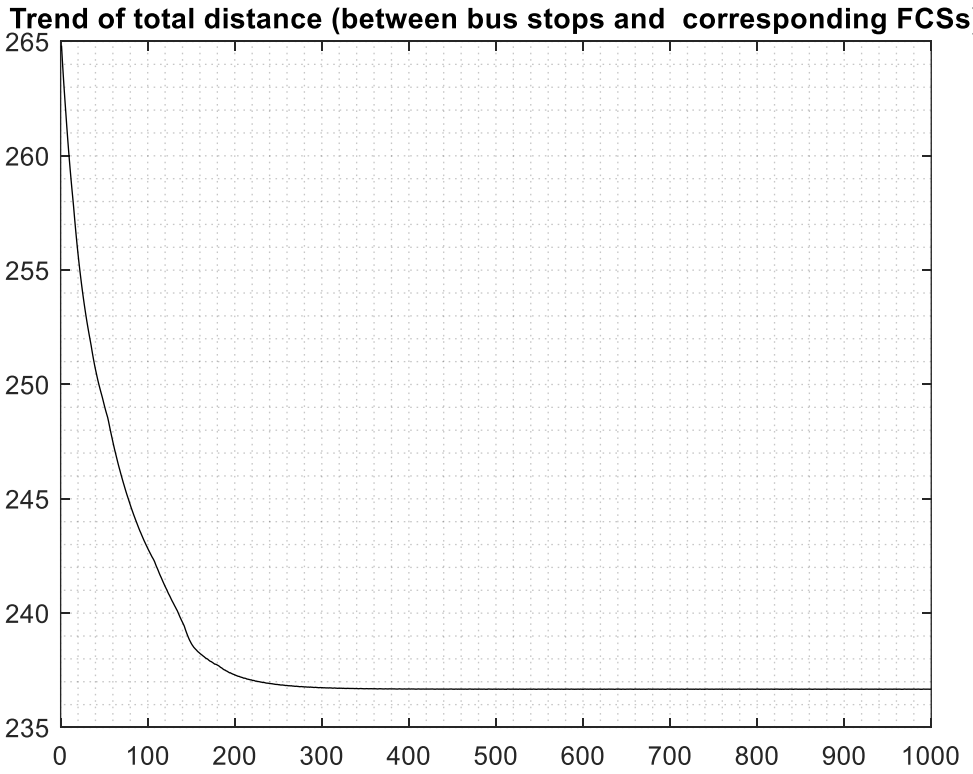

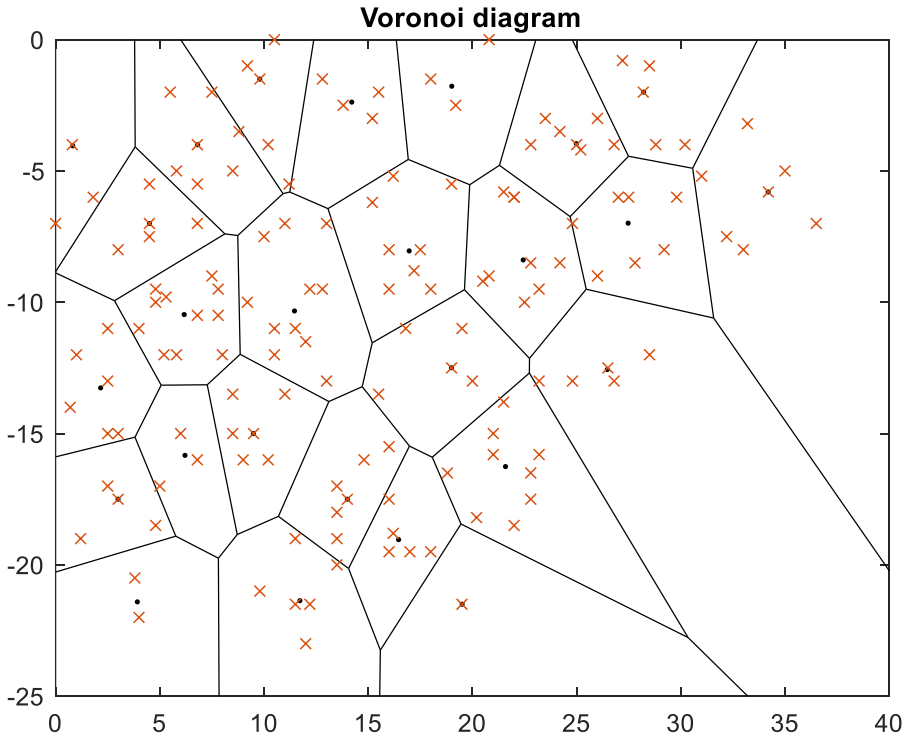

Figure 21- Trend of total distance with HDG [km] and final positions

In table 3 numerical results reflects the real improvement of new EHDG technique. It has a greater computational cost, but on the other hand it is more effective.

Method	Optimal target function value [km]
Descent gradient	243.6
Genetic algorithm	272.4
EHDG	236.7

Table 3- Target value in three different simulations

Results show that DG minimization is better than GA and target function value is actually 10% lower. Practical values display that total distance between all bus terminal stop and their relative FCS is about 272 km with genetic algorithm work.

Descent gradient optimization places station points in a better way and total distance value decreases to 243 km.

The implementation of the new algorithm moves a little final positions and target equation value drops down to 236 km which represent a little improvement in a single route but that is a great work and saving in the long time.

4.3) FUTURE SCENARIOS RESULTS

After the optimization problem, different scenarios can be illustrated to underline the real cost savings. The optimization of this work doesn't involve deeply the type of bus battery or other characteristic of the vehicle. The only step that influence the total algorithm is in equation (3), where it is important the number of vehicles and the time that need to charge that reflects mainly on the type of battery involved, that can be LTO or LFP (slow or fast charge). First part of the work, in the end, can be studied and changed to find the optimal number of stations for the application of cars, too. Successive and main part of the work will be the same since it works just with points in an area.

In order to have some practical values about energy and economic savings, seven different electric consumptions of existing bus are studied. These categories involve greatest part of electric bus flow and can sign a realistic and actual idea of the savings. The trend of the cost they spend to go from bus stop to FCS outputs the goodness of previous work. A mid-peak cost of energy (0.095 $/kWh) is considered as average in this study, but a smart use of charging time can be an additional saving source.

The bus network schedule clears up the number of routes of each bus and then it is shown the annual cost that buses have to sustain only to go from their final stop to nearest electrical DC fast charging station during working hours.

After the optimization, various consideration take place. First of all, money saving between initial and regular positions and final and best ones is about 35%. If considerations are about genetic algorithm and EHDG method (that starts with GA final positions), improvement is about 13%. Note that results in the table are costs about a single route of all bus flow, but every day there are 7 routes and in a medium or long time it is a great economic saving. Figure 22 shows the trend of the costs of one year's work and it is evident to note that buses that consumes 2 kWh/km (one of the most diffuse) can save about 60 k$ every year in actual network.

In table 4, each value of the table is referred to the sum of all buses for one route. With the application of this technique, in each case, final costs reduce more than 1/3 every year, which leads to a very significant annual saving.

Bus consumption [kWh/km]	Target function [$]			
	Before optimization	After Genetic Algorithm optimization	After Descent Gradient optimization	After EHDG optimization
1	34,2	25.9	23.1	22,5
1,1	37,6	28.5	25.5	24,8
1,2	41,1	31	27.8	27,0
1,4	47,9	36.2	32.4	31,5
1,6	54,7	41.4	37	36,0
1,8	61,6	46.6	41.7	40,5
2	68,4	51.8	46.3	45,0

Table 4- Target function in four different cases

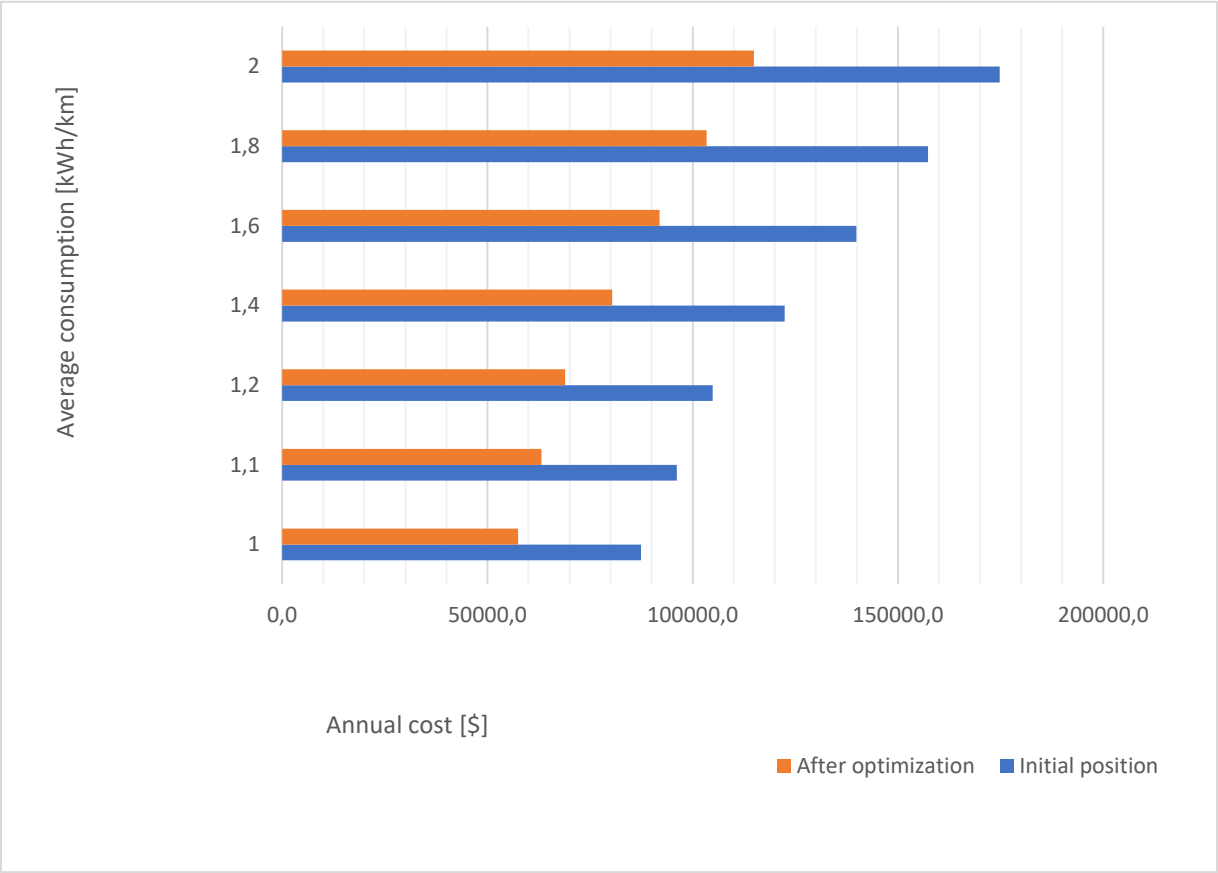

Figure 22- Average consumption[kWh/km]

5) OPTIMIZATION OF FFCS CONTROL SYSTEM

Second part of the thesis is an optimization work applied in the control system of the fast charging station infrastructure.

Flywheel Fast Charging Station (FFCS) is used to provide reliable fast charging infrastructures for e-Buses and EVs using flywheel technology. Thesis presents an advanced computational intelligence technique based on Artificial Immune System (AIS) to improve the performance of FFCS to support transportation electrification. FFCSs are optimally integrated with utility grid networks, where they offer balancing loads and protecting the grid from any collapse. In addition, FFCS can offer significant reduction of energy costs and maximize energy supply from renewable sources. Artificial Immune System (AIS) is an advanced optimization technique that is proposed to tune the optimal dynamic parameters correlated to PID control of FFCS.

Based on those mentioned attributes, Flywheel Fast Charging Station (FFCS) is proposed to provide fast charging capabilities for electric vehicles and other transportation systems by utilizing the dynamic response of flywheel systems.

Present infrastructure shows the internal design of the proposed FFCS that offers the following key advantages: handle peak demand, store energy from renewable sources, avoid grid overload, and reduce charging cost [24] [25]. Energy storage system can handle those mentioned objectives, in particular this paper studies flywheel energy storage system driven by induction machine, that is the most suitable technology in this field at this moment.

Direct torque control (DTC) control is applied on FFCS to provide a better dynamic performance and to regulate torque value. To enhance the dynamic performance and increase the output parameters of traditional DTC, PID block will be implemented and tuned by minimizing the driven error signal with the application of an advanced computational intelligence technique, called Artificial Immune System (AIS). Detailed procedure of AIS is the core business of future work of this thesis.

6) FAST CHARGING SYSTEM DESIGN

The physical structure of e-bus DC fast charging station [26] includes:

- A three-phase AC/DC/AC converter, with a common DC bus that is linked both to grid and flywheel interfaces.

- DC/DC converters to connect the station to the bus chargers that represents the load of the system. Usually it provides unidirectional current flow from grid to system to reduce the degradation of the bus battery;
- The core of charging stations is the flywheel, which acts as a primary energy storage system.
- The flywheel model contains energy storage subsystem, DTC with SVPWM subsystem, voltage/frequency control subsystem, Permanent Magnet Synchronous Motor (PMSM), and power control system.

The simplified model of the proposed Flywheel Fast Charging station (FFCS) is presented, as shown in figure 23.

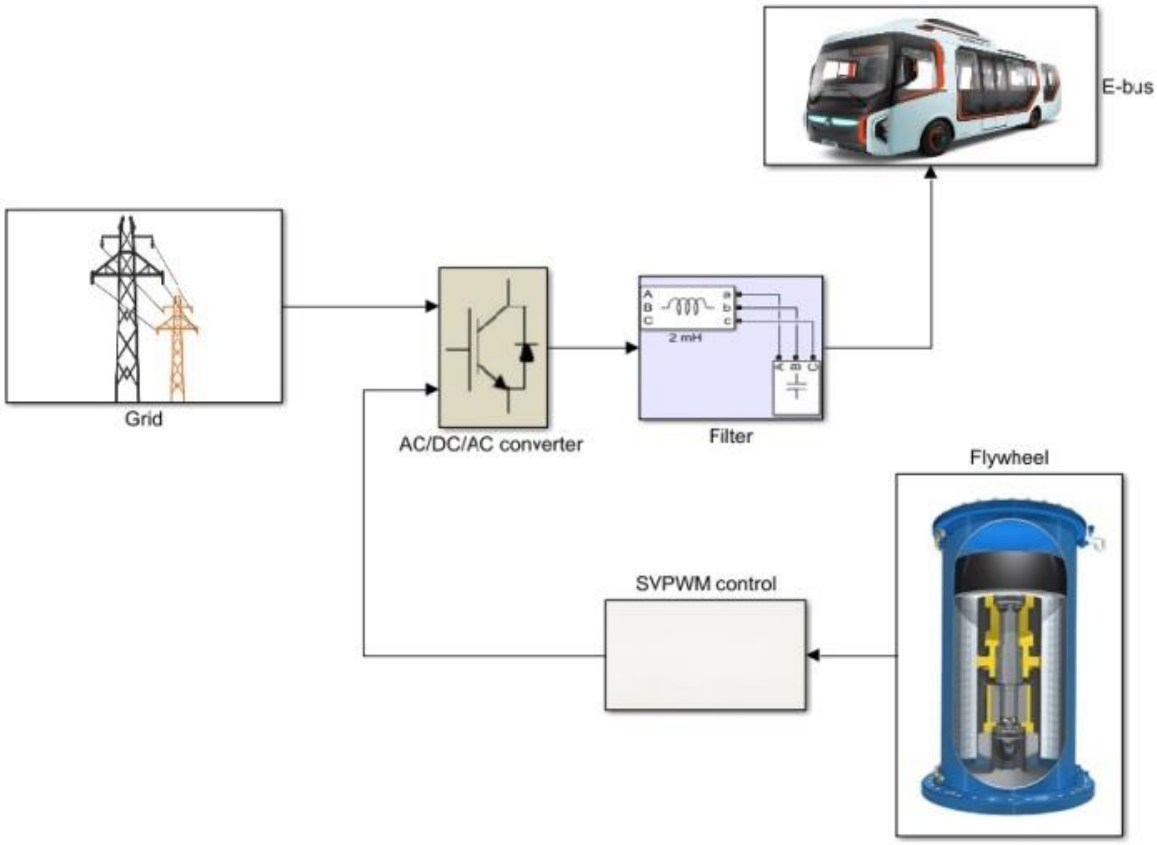

Figure 23- Simplified model of FFCS

The selected transportation infrastructure is for e-buses, which will reflect in real-world case of bus network at downtown Toronto city with simulated bus stops at distances of 3 km, and with peak power 1.5MW and 10.06 kWh for the longest trip/stop.

6.1) FLYWHEEL MODEL

Energy storage systems are integrated within the charging stations to balance electricity supply and demand. In addition, they are considered as major element to enhance the operation reliability and quality of utility grids [26]. Flywheel technology has recently gained great attentions where it has various impacts and benefits due to its fast-dynamic response at charging and discharging cycles with significant characteristics of high operational lifetime at remarkable round-trip efficiency [27].

Table shows a comparison between different types of energy storage systems that confirms the fast charging capability of flywheel storage system [28].

	Flywheel	Ultra-capacitor	Li-ion Batteries
Power (kW)	2-500	5-1000	-
Energy (Wh/kg)	15-150	0.5-4	3-100
Power density (Wh/kg)	900-20000	50-3000	100-1000
Energy Density (kWh/m^3)	6-100	0.8-4	80-200
Power Density (kWh/m^3)	0.3-40	0.3-1	0.4-2
Maximum Cycles	>100000	>100000	3000
Discharge time range	4-60s	1-60s	10s-1h
Life Expectancy (hrs)	175000	100000	17520-26280

Table 5- Energy storage systems

Energy storage system is a topic that is continuously being developed; battery energy storage still has some problems due to degradation of battery influenced by the frequency of charging/discharging cycles. For that reason, it is proposed to apply flywheel energy storage, that is more advanced and reliable technology with respect to others in this field.

Flywheel Energy Storage accelerate an internal rotor and then conserve energy as rotational energy. During charging phase, it works as motor and usually absorbs current and accelerate its rotor that is

flywheel itself. When it works as generator, system give power to third component and rotor decelerates [29].

Technology is developing year by year and actual great performances are a result due to fiber-carbon composites material that form the rotor (instead of steel material). Flywheel in addition rotates with high-speed suspended by magnetic bearings (instead of mechanical ones) in a vacuum space to reduce frictions and additional losses.

Most uses are in automotive field since second half of 1900 in order to substitute chemical batteries in the shift from traditional to electrical vehicles with a lot of advantages.

Another field application is grid energy storage, that is applied in this thesis [30]. Flywheels are used as fast-response reserve to balance drop between demand and production. In addition to fast availability another great advantage is to buy power at off-peak hours. All these opportunities will reflect on energy savage and consequently on economic side, too. Actual greater storage field are in Ontario, Canada and in NY, with a plant power of 20 MW.

Energy internally stored in considered system is:

$$E = \frac{1}{2} I \omega^2 \tag{21}$$

Where I represents the inertia moment of the rotor and ω is the angular velocity.

A cylinder flywheel is considered and will lead to a moment of inertia as follow:

$$I = \frac{1}{2} \pi \rho h (r_0^4 - r_i^4) \tag{22}$$

Where ρ is mass density, h is the length and r_0, r_i are outer and inner diameter of the flywheel, respectively.

The description of electrical system is:

$$\frac{d}{dt} i_d = \frac{1}{L_d} v_d - \frac{R}{L_d} i_d + \frac{L_q}{L_d} p \omega_r i_q \tag{23}$$

$$\frac{d}{dt} i_q = \frac{1}{L_q} v_q - \frac{R}{L_q} i_q + \frac{L_d}{L_q} p \omega_r i_q - \frac{\lambda p \omega_r}{L_q} \tag{24}$$

$$T_e = 1.5\, p\, [\lambda i_q + (L_d - L_q) i_d i_q] \tag{25}$$

where, L_q and L_d represent inductances on q and d axis, R is the resistance of the serpentine of the stator, i_q and i_d are currents on q and d axis, V_q and V_d represent voltage on q and d axis, ω_r is the angular velocity of the rotor, λ is the magnetic flux caused by the permanent magnet, p is the number of pole pairs and T_e is the electromagnetic torque and its sign indicates if flywheel is working as motor or generator.

Then mechanical system is defined as follow:

$$\frac{d}{dt}\omega_r = \frac{1}{J}(T_e - F\omega_r - T_m) \tag{26}$$

$$\frac{d\theta}{dt} = \omega_r \tag{27}$$

Where J and F represent the combined inertia and viscous friction between rotor and load, respectively, while θ is the angular setting of rotor and T_m is the mechanic torque of the mast.

To calculate the total amount of force that the bus must overcome for acceleration to the consumed power, the following equation is used:

$$F_t - F_r - F_g - F_c = m_e a \tag{28}$$

Where:

F_t is the tractive force from the traction system in N;

F_r is the running resistance force in N;

F_g is the resistance force due to gradient in N;

F_c is the resistance due to the curve in N;

m_e is the effective mass of the bus in kg;

a is the total acceleration in m/s^2.

Effective mass can be calculated using:

$$m_e = m_t(1 + \mu) + m_p \tag{29}$$

Where:

m_t is the tare mass in kg;

μ is the rotary allowance (typically 5-15%);

m_p is the payload in kg.

Running resistance can be calculated using:

$$F_r = A + Bv + Cv^2 \tag{30}$$

Where:

A is the rolling resistance coefficient;

B is the bearing or viscous friction coefficient;

C is the aerodynamic drag coefficient;

v is the current velocity in m/s.

Gradient Resistance can be calculated using:

$$F_g = g(m_t + m_p)sin(\alpha) \tag{31}$$

Where α is the incline angle.

Curvature Resistance can be calculated using:

$$F_c = (m_t + m_p)g * \frac{1}{1000} * \frac{700}{R} \tag{32}$$

where, R is the curvature radius (meter).

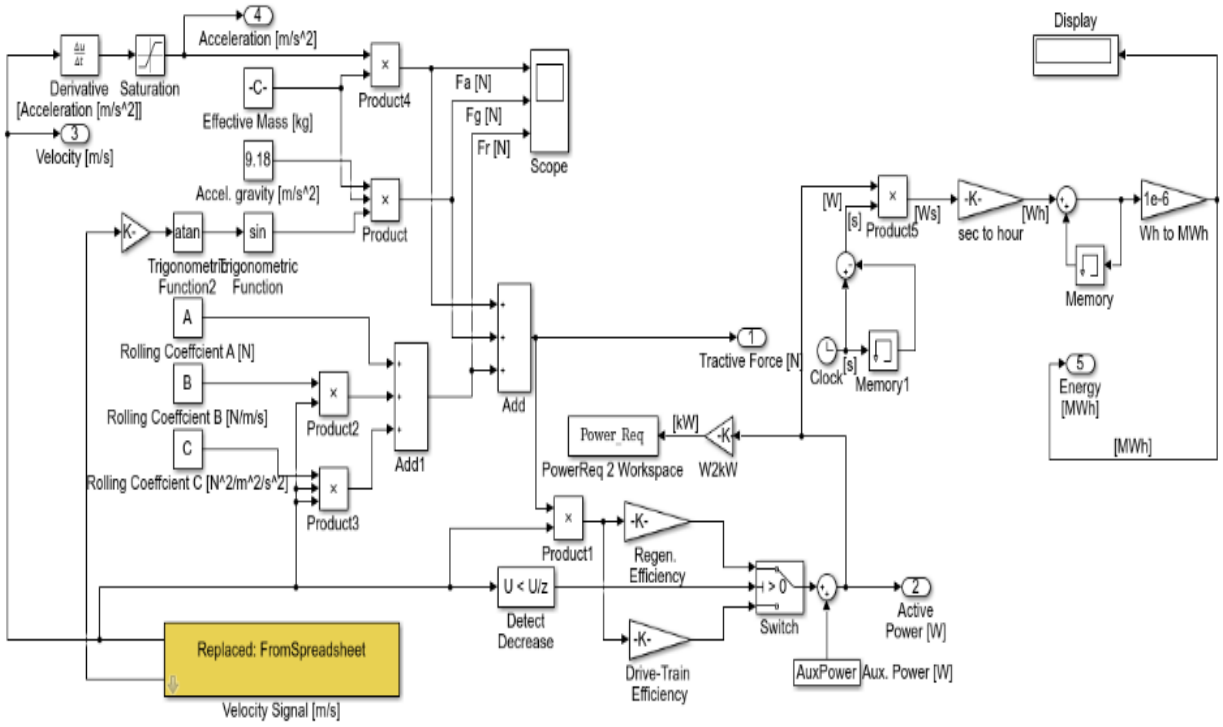

Figure 24- e-BUS SIMULINK model

6.2) SVPWM CONTROL

Components where this control is involved in is the voltage source inverter. Their task is mainly to convert from DC to AC and provide sinusoidal voltage waveforms as requested from modern power electronics-based devices.

Flywheel model is a suitable device that need the voltage inverter for its variable voltage (caused by variable speed) application. To obtain better performance of required voltage as output of the inverter the most used and suitable technique is Pulse Width Modulation (PWM).

In this control the ac output voltage is the result of the on-off work of proper switch.

Actually, it is one of the most used control methods and its result are:

- The desired output voltage is obtained without additional components;
- High voltage is performed without harmonic distortion (in particular low harmonics).

In particular the work of actual thesis focuses on space vector method (SVPWM) that is suitable for three phase inverters [31]. The name of this technique come from the use of vectors to represent space voltage in the α-β plane.

Space Vector PWM (SVPWM) plays a major role in flywheel control where it is utilized in the current FFCS design [32]. Its goal is to provide a better dynamic performance and higher output variables: speed, energy and torque to the flywheel.

This technique starts using Clarke-Park (CP) transformation, where three phase voltage and current are converted into a two-dimensional rotating reference d-q frame. Three phase voltage is represented as follow:

$$V_a = V_m sin\omega t \tag{33}$$

$$V_b = V_m \sin(\omega t - {}^{2}/_{3}\,\pi) \tag{34}$$

$$V_c = V_m \sin(\omega t - {}^{4}/_{3}\,\pi) \tag{35}$$

In particular, following figure illustrates how described CP transformation works.

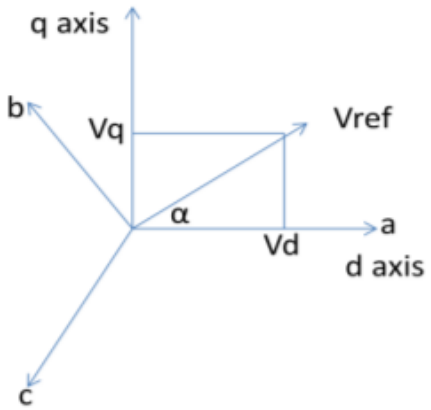

Figure 25- CP transformation

$$V_{\mathrm{d}} = {}^{2}/_{3}\,[V_a \sin(\omega \mathrm{t}) + V_b \sin(\omega \mathrm{t} - {}^{2}/_{3}\,\pi) + V_c \sin(\omega \mathrm{t} + {}^{2}/_{3}\,\pi)] \tag{36}$$

$$V_{\mathrm{q}} = {}^{2}/_{3}\,[V_a \sin(\omega \mathrm{t}) + V_b \cos(\omega \mathrm{t} - {}^{2}/_{3}\,\pi) + V_c \cos(\omega \mathrm{t} + {}^{2}/_{3}\,\pi) \tag{37}$$

$$V_0 = {}^1/_3 (V_a + V_b + V_c) \tag{38}$$

Successive step is the calculation of reference value and angle of the output through following system.

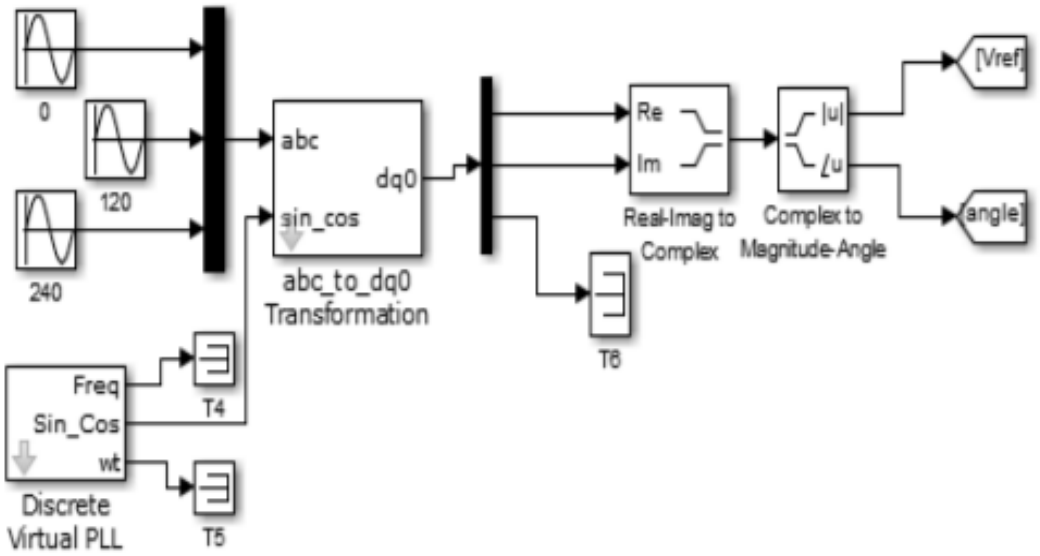

Figure 26- SVPWM system

Following three phase voltage source inverter (VSI) has 3 upper switches and 3 complementary lower switches. The number of combinations to obtain the correct value is eight: 000, 001, 010, 011, 100, 101, 110, 111 (0 represents lower leg and 1 upper leg).

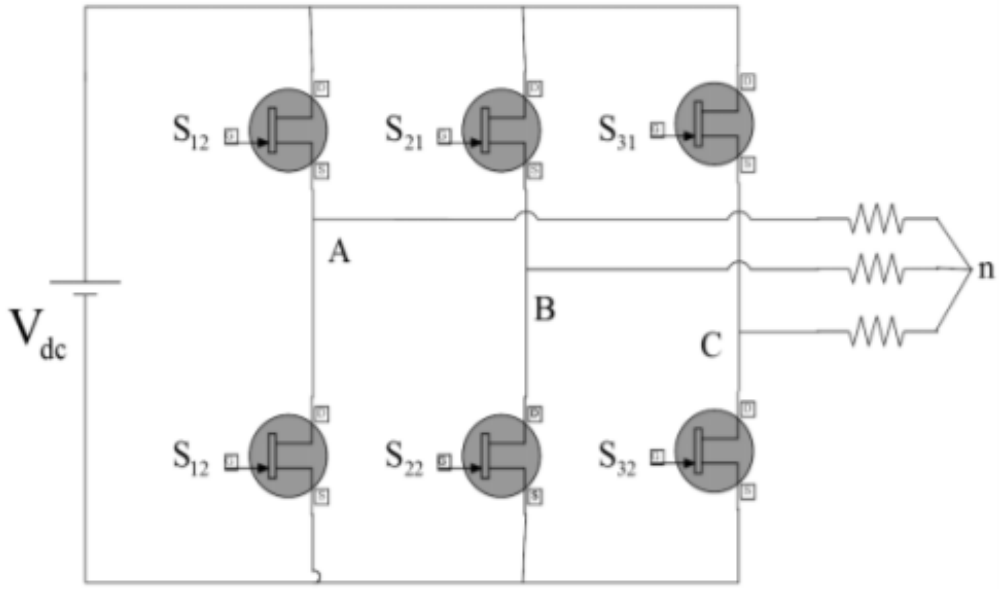

Figure 27- Three phase VSI

As showed in following figure, two out of eight states are null and the other six are active. V0 and V7 are zero vectors and don't supply signal to the load.

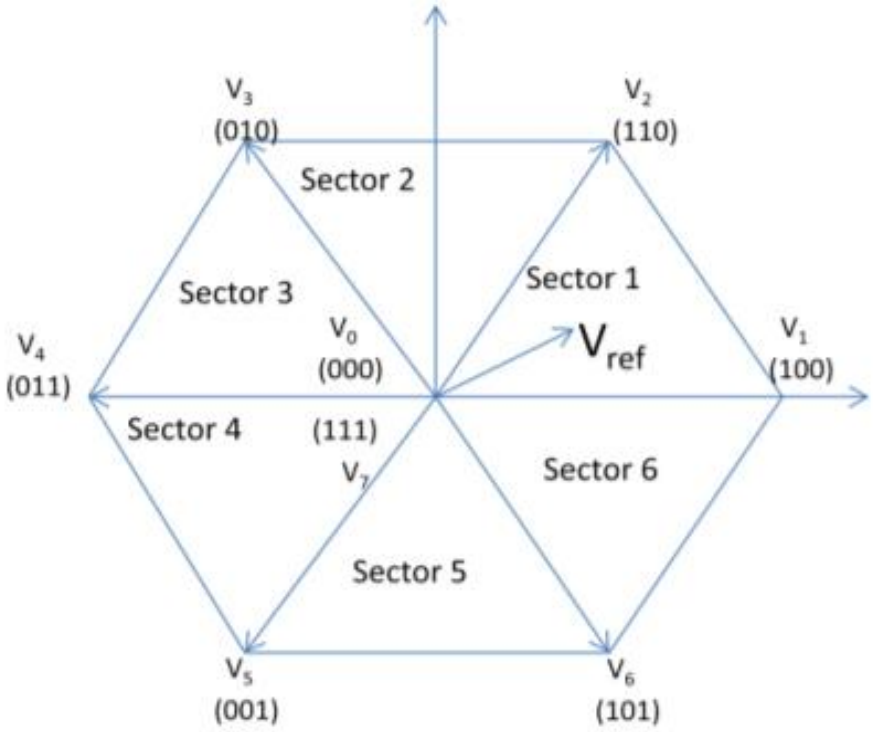

Figure 28- Hexagonal representation

The aim of this hexagon representation is to estimate reference output vector using the eight states. Work starts with the individuation of the correct sector and then the application of V_1, V_2, V_z vectors for a certain time will generate correct pulses to drive the switches of the inverter.

6.3) DTC-SVPWM CONTROL:

Switching system previously described can lead to an amount of harmonics that will cause others power losses in the motor. In addition to losses also torque and mechanical pieces can have damages and problems.

Direct Torque Control is a suitable control strategy used to control the torque and reduce the total harmonic distortion (THD) in a three-phase motor [33]. It was born thanks to Takahashi and Nouguchi in 1986 and in parallel with the work of Depenbrock in 1988. During second half of 90s there were first industrial applications based on DTC system.

In last years, it is one of the most interesting control strategies for induction motor supplied by a voltage source inverter because it is independent of parameters of the machine rotor.

The main disadvantage of this technique is the presence of torque and flux ripples.

DTC drive configuration starts with the calculation of motor flux and torque with motor voltages and currents values. In particular, stator flux linkage is calculated integrating voltage vector while torque is the product of stator flux and motor current.

Comparison between stator flux and torque values with their reference values will probably lead to an error value due to a difference in the estimation. In particular, flux and torque ripples come from the incapability of the VSI to create precise output voltage vector. Hysteresis comparator is the adopted technique to reduce the error band. Control system also called bang-bang control turns transistor on and off in order to reach correct band of the value through the work of a voltage vector selector.

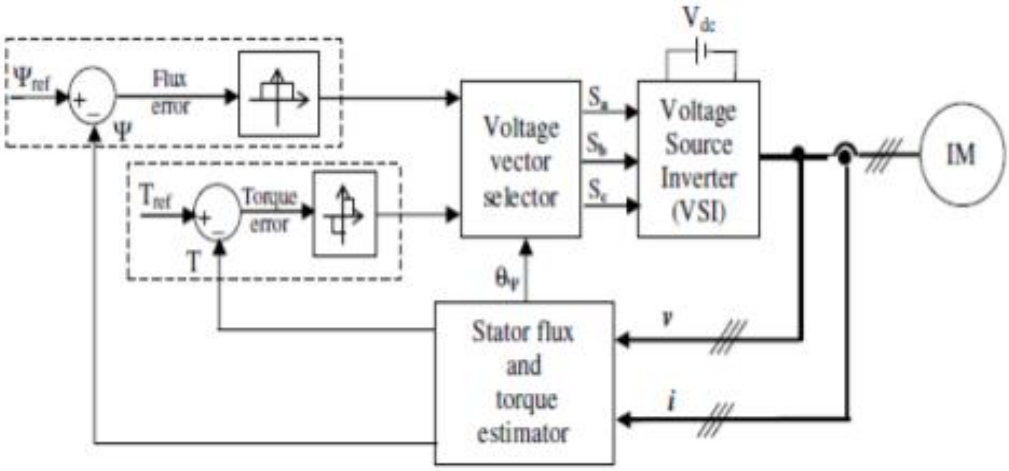

Figure 29- Traditional DTC representation

One of the most enhanced technology actually used provides the application of the space vector pulse width modulation (SVPWM) in the direct torque control (DTC) [34]. In particular the work of the hysteresis control is done by PID controller.

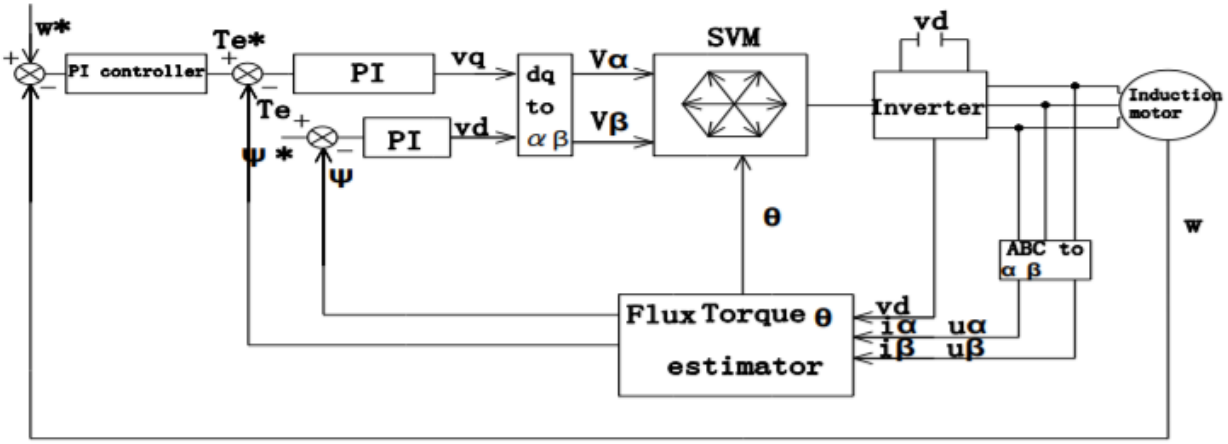

Figure 30- DTC-SVPWM representation

Comparison with described SVPWM shows in figure 30 that output of PI controllers for torque and flux are d-q components of stator voltage previously cited in the work of SVPWM control [35].

Next step is similar to previous one: system calculates voltage and current in order to obtain stator flux (φ) value and subsequently electromagnetic torque (T_e) through following equation:

$$T_e = \frac{2}{3} p(\varphi_{s\alpha} i_{s\beta} - \varphi_{s\beta} i_{s\alpha}) \tag{39}$$

Comparison with reference flux (φ') and torque (T'_e) values generates command voltage components in a synchronous reference system (following equations) V_d, V_q.

$$V_d = \left(K_{p\varphi} + \frac{K_{l\varphi}}{S}\right)(\varphi^*{}_s - \varphi_s) \tag{40}$$

$$V_q = \left(K_{pt} + \frac{K_{lt}}{S}\right)(T^*{}_e - T_e) \tag{41}$$

Precision of these values is the core business of the application of this technique as they are involved in the generation of pulses that drive the inverter to have lower torque and flux ripple in the output.

Command voltage components are input values for SVPWM that create the gate pulse using the voltage source inverter (VSI). Control system transforms also back values to the three-dimensional axis with the work of the inverse of the Clarke-Park transformation.

Also, PID controller operates on the resultant total power between the grid and the flywheel, measured by the error signal between the reference value and the measured one.

7) PID CONTROL

7.1) THEORETICAL APPROACH

A control system is a fundamental process that is involved in all devices starting from simplest house heating system to more complex industrial process. It is an ensemble of functions and physical components that control the process and attend on it in order to have as output of the system the desired one called set point value. The final control element (FCE) is the physical component that acts finally on the manipulating variable. Described block of function and components is the so-called control loop.
Controller works by calculating continuously an error rate e(t), that is the difference between a theoretical set-point (SP) and the real simulation value (SV); then it works on it basing on the kind of control. ON-OFF control is the simplest one, but in this thesis PID control works on the studied device that offer a wide range of solution with higher efficiency.
A proportional–integral–derivative (PID) controller is actually one of the most used and studied control technique [36]. In particular it applies a continuously a modulated control based on proportional, integral, and derivative terms.
Minimizing the error with PID control means optimize the control function u(t) defined as follow:

$$u(t) = K_p\, e(t) + K_i \int_0^t e(t')dt' + K_d \frac{de(t)}{dt} \tag{42}$$

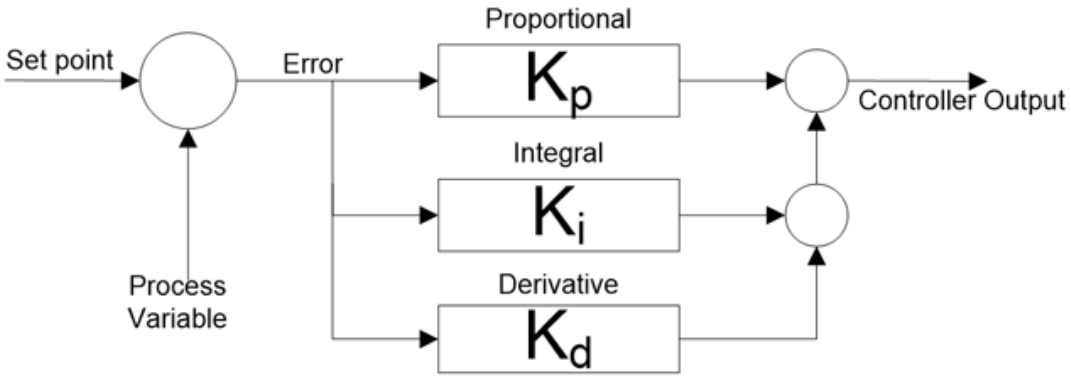

Figure 31- PID controller system

Proportional, integral and derivative terms are sequentially applied to the error function in order to decrease its value u(t).
Term K_p is simply proportional to the $SP - PV$ error e(t).
Integral coefficient K_i works studying past value of the errors e(t) and integrate these values on time. In this way the residual error resulting after the application of proportional part of the controller can be reduced.
Term K_d works estimating the future trend of error value and in this wat tries to lead the function to an optimal value.

8) AIS ALGORITHM

Let see in this paragraph how Artificial Immune System (AIS) works. It is one of the most studied and reliable meta heuristic techniques and is a control mechanism that draws inspirations from theoretical immunology system and observed immune functions, and that can be applied on control problems in various fields.
AIS based algorithms are divided into two major categories: population based and network based. The difference between these two classes is that the first one follows clonal selection and negative selection concept, while the other is based on immune network theory. This thesis puts its focus on clonal selection theory in order to optimize PID control [36].

8.1) CLONAL SELECTION

Clonal selection is a scientific immunology theory that exposes the immunity response from B and T lymphocytes against antigens invasion in a process denoted as “affinity maturation”.
Studies started with Frank Macfarlane Burnet in 1957 in order to find an answer to the different ways of antibodies creation during antigens response. First scientific evidence came in 1958 when Gustav Nossal and Joshua Lederberg showed that B cells always produce one antibody.
General concept is that cells able to proliferate are those that recognize antigens (i.e. external pathogens, bacteria, fungi, viruses, etc). Selected cells are subject to a maturation process of the affinity compared to the selective antigen [37].

8.1.1) CLONAL SELECTION THEORY

Antigens are molecule recognized by immune system and when a human body is exposed to an antigen, B lymphocytes produce antibodies that are specific to this particular antigen. Now clonal selection process starts: T lymphocytes help B cells to proliferate into plasma cells (clone progeny of starting cell) in a division process called mitosis. Some B cells differentiate into long-lived memory cells that will have a higher affinity with antigens in a future response. They circulate into the blood and will have important role in a future response. Other B cells differentiate in other plasma cells and secrete antibodies into circulation.

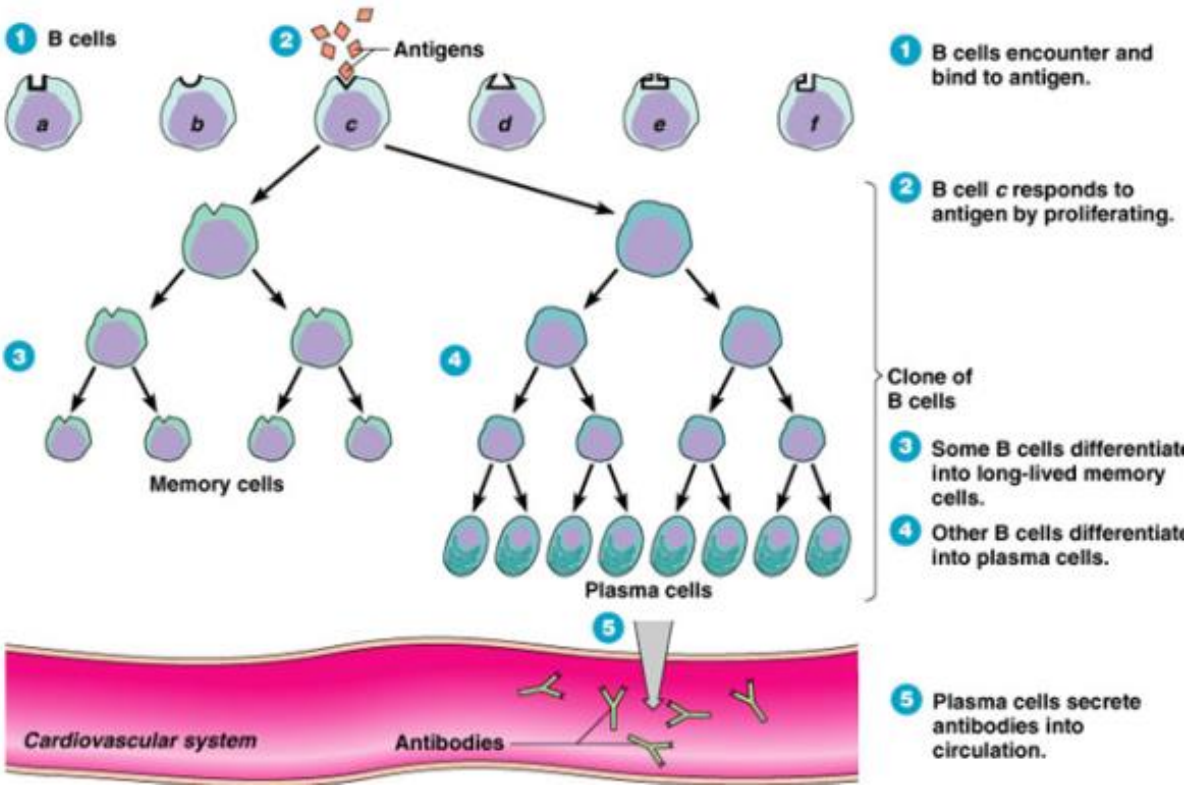

Figure 32- Antibody evolution

8.1.2) AFFINITY MATURATION

The presence of memory cells improves antibody response in future situations. This phase is the core of affinity maturation theory: antibodies in memory have a higher affinity with respect to primary response ones and this point reflects on lower delay time and higher number of amounts during the intervention (

figure 33) [38]. Step by step the binding of antigens and antibodies is different and this represent the maturation of immune response. Improvement process expects that antibody Ab suffers mutations with casual changes on its receptors after primary response. Successive antibody with lower affinity is discharged, while a greater affinity represents an intermediate step to get to global optimum Ab*.

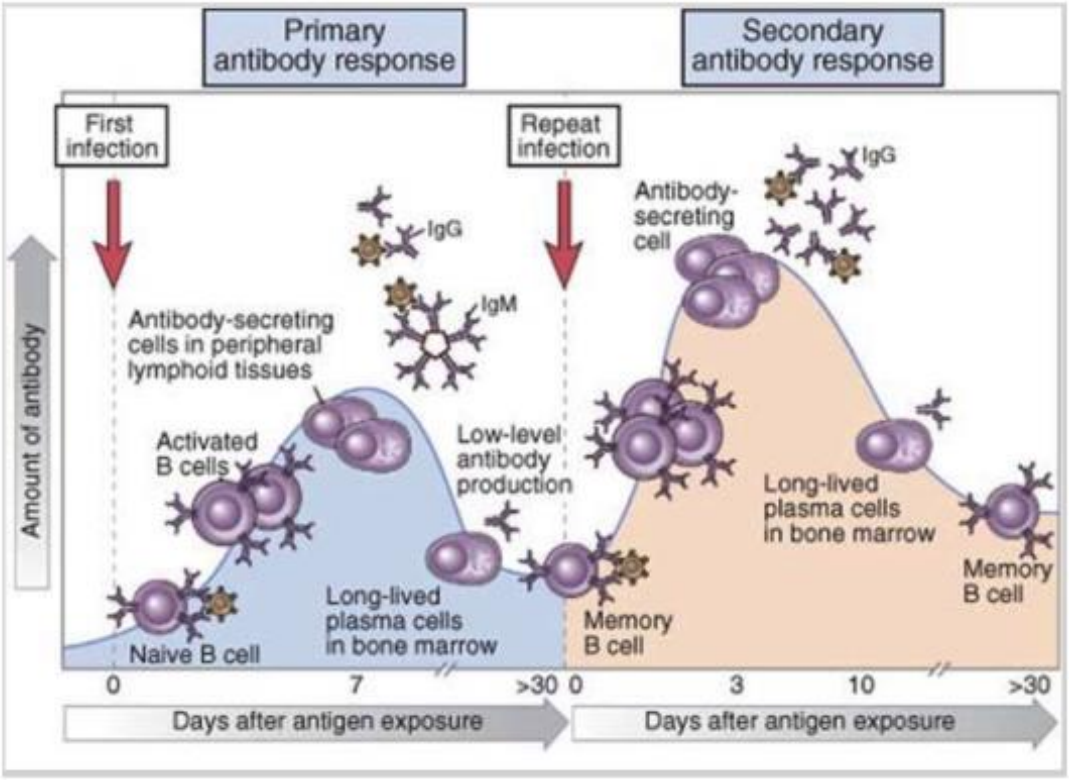

Figure 33- Affinity maturation

9) AIS COMPUTATIONAL ALGORITHM

Starting from previous scientific theory, CLONALG is an algorithm born to apply AIS theory to an optimization problem basing on some of the previous focus points:

- Reproduction of cell through cell division (mitosis);
- Selection through Ab – Ag interaction affinity;
- Variation with somatic hypermutation.

Algorithm takes into considerations in each step only best solutions to reduce computation cost and space.

CLONALG is a computational algorithm that works similarly to artificial immune system [39].
In immune theory AIS optimize the interaction between antigens and antibodies through successive infection and in the same way computational AIS algorithm is useful to optimize a general problem called by a function, as in this thesis.
It is useful to see in parallel the evolution of AIS theory and AIS computational algorithm: the optimization algorithm starts by defining an abject function f(x) that has to be optimized (minimized or maximized) and in the immunology word it represents antigens.
Successively algorithm works creating some candidate solutions represented by antibodies. They are represented by 8-bit string and their affinity with main function is calculated.
Successive step is the proliferation of B cells that create clone cells. The algorithm in particular needs memory cells that are useful to find global optimum solution. Antibodies with higher affinity now have a major role during proliferation process in the simulation.
The string representation of cloned cell is the result of the process of somatic hypermutation.
Finally, new generation is a perfect mix of the best old parents and the best cloned cells. In this way the solutions with high affinity is the best for the problem and it can be useful, in addition, to calculate the local minima.
Steps that MATLAB algorithm follows to reproduce AIS theory for the optimization of a function f(x) [40] are:

- Function and constraints definition:

In the immunology word the global optimum is when antibody perform optimally against an antigen. Before starting the parallel work with the computational algorithm, cycle needs to define the function to optimize and its constraints that will define the end of the work. In the work of this thesis they are the maximum number of cycles and the error.

$$F(x) = \sum_{t=0}^{T} (e(t))^2 \tag{43}$$

$$x_l < x < x_u \tag{44}$$

- Evaluation of the antigen:

In this thesis the aim is to optimize an error function and this is the object antigen of AIS theory.

- Initialization of a population of antibodies:

Antibodies of AIS process are the probable solution of the optimization problem function. In particular the algorithm represents each variable as a string with 8 bits of binary code.

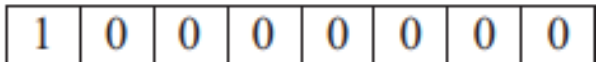

Figure 34- 8 bits binary code

First population defines the primary response in the immune system and is created randomly following the constraints defined in the problem.

- Calculation of the affinity for each generation of antibodies:

Antibodies represent a candidate solution for the function and they are ordered after the performance of their affinity evaluation.

$$f = \frac{1}{1 + f(x)} \tag{45}$$

- Proliferation step:

Starting from classification based on affinity evaluation, the best 50% of antibodies are parents of successive generation of clones. Antibodies with high value of affinity will have greater number of clone strings, while lower affinity price has less copy. N_c comes from analytical expression and represents the number of clones generated:

$$N_c = \sum_{i=1}^{N} [\frac{\beta N_b}{n_i}] \tag{46}$$

Where:

- N_b= is the strength of starting antibodies;
- n_i is the i^{th} antibody in its population;
- β is the multiplying factor;

- Somatic hypermutation:

Bits of the strings that represent the clones suffer the process of somatic hypermutation. AIS algorithm provide a smart mutation to the new generation of antibodies: those with higher affinity have a lower probability of mutation and vice versa. The rate of mutation for each antibody is analytically calculated:

$$\sigma = e^{-\delta f} \tag{47}$$

Where:

σ= rate of hypermutation

δ= decay control factor

f= affinity

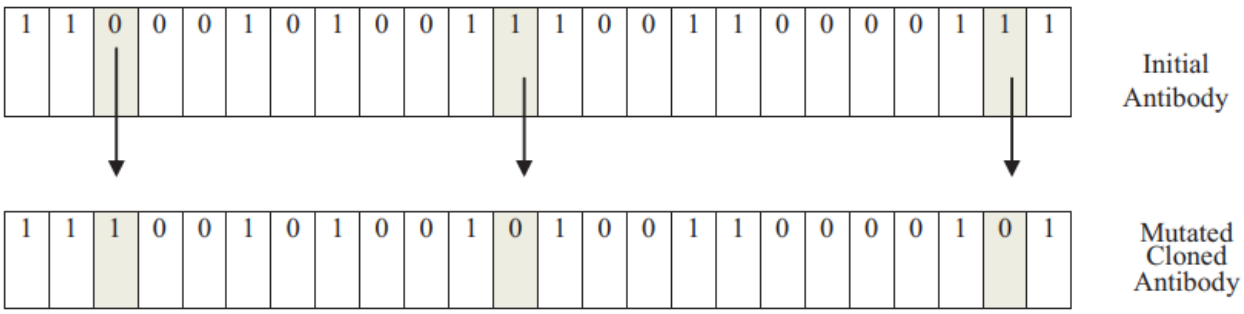

Figure 35- Mutation process

- Selection of new population:

Fresh population of antibodies matches with antigen and affinity of each element is performed. Then the best half of antibodies is put together with the best half of old parents and these elements constitute new population in next step.

- Evaluation of the optimization function value:

If constraints evaluated at the beginning of the simulation are reached, simulation ends. Otherwise cycle restarts and new generations of antibodies (with high performance step by step) are created until the positive check of the coverage criteria.

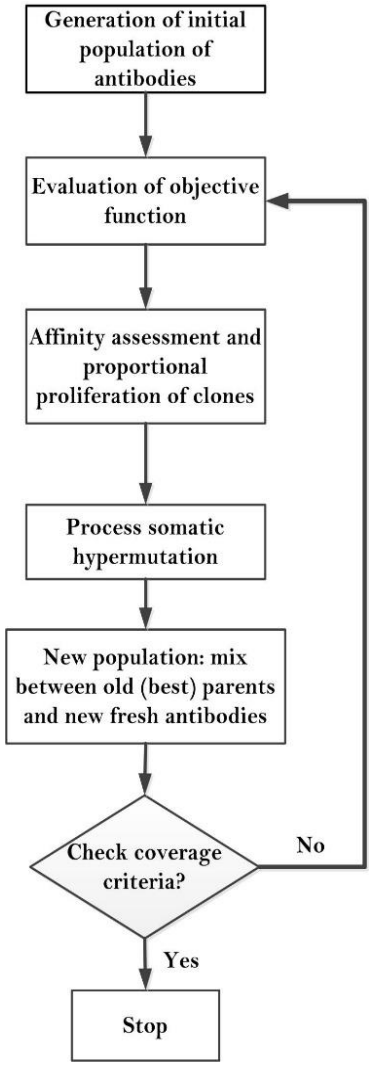

Figure 36- AIS computational algorithm

10) ENHANCED PID CONTROL APPLICATION

After traditional application, controller subsystem is improved using a PID tuned AIS mechanism defining, first of all, a fitness function as affinity measure for the simulation and then a stop principle, for example a maximum number of generations. In this case the fitness function to minimize is the error previously mentioned u(t) and the main goal of this method is to find new variables K_p, K_i, K_d improving control.

10.1) CASE STUDY PARAMETERS

Proportional-Integral-Derivative (PID) controller is built as an integrated component to control the flywheel where PID is linked to the input signal of SVPWM. This will lead to improved performance compared with the traditional DTC control techniques [41]. In fact the FFCS control performance is improved using a PID, which is tuned with Artificial Immune System (AIS) technique.

In particular the aim is to minimize the involved error in the DTC system with the calculation of K_p, K_i, K_d parameters.

These three parameters represent the antibodies of the AIS algorithm application and their structure is:

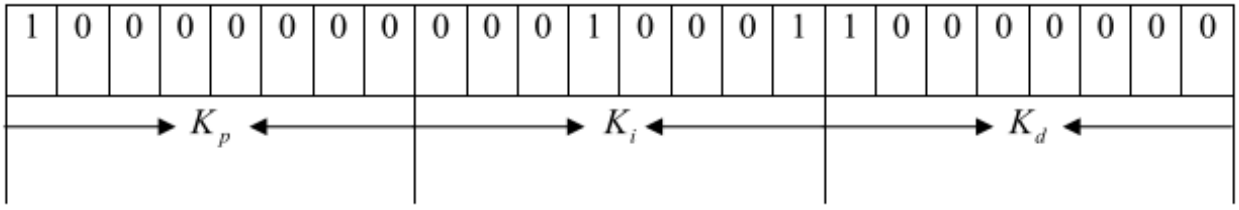

Figure 37- PID parameters representation through 8-bits binary code

The fitness function is defined to measure the performance during the simulation process and is the error value direct measured between real and theoretical one in DTC. It is additionally linked with stop criteria, such as maximum number of generations.

Some parameters are defined in MATLAB/SIMULINK program to follow the AIS computational algorithm described in chapter:

Parameter	
Population size	50
Clone size factor [%]	20
Maximum number of generations	50
β	1
δ	10^4

Table 6- Main AIS optimization parameters

The selected case studies are based on infrastructure for e-buses at downtown Toronto with simulated bus stops at distances of 3km, and with peak power 1.5MW and 10.06 kWh for the longest trip/stop.

10.2) SIMULINK STATION DESIGN

Electrical schematization of FFCS is implemented in SIMULINK model and contain grid and flywheel side connected with an AC/DC/AC converter and a filter. Output of the converter is connected to the external bus battery. Core business of actual thesis is the DTC-SVPWM control for flywheel and the power control in the power connection between grid and flywheel [42]. Following figure shows described components.

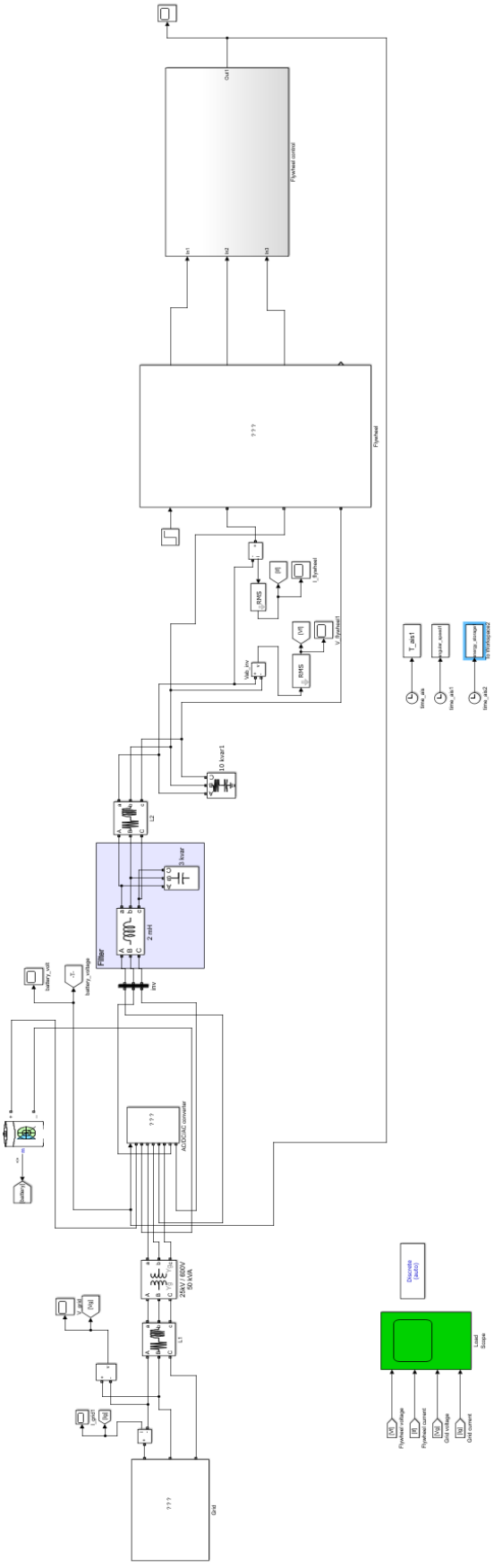

Figure 38- FFCS SIMULINK design

Electrical parameters set for the correct operation of the station are following and are imposed to the Simulink model.

Electrical parameters	
DC bus capacitor	2.2 mF
Line inductor	3.8 mH
Line resistor	0.2 Ω
DC bus voltage	650 V
Distribution Grid voltage	325 V
Flywheel parameters	
Stator inductor	10.5 mH
Rotor inductor	10.8 mH
Total leakage coefficient	0.0566
Rotor resistance	2.37 Ω
Stator resistance	1.95 Ω
Flywheel inertia	10.2 kg m^2

Table 7- Grid and Flywheel parameters

Following figure represents schematization of DTC improved with the help of SVPWM and its output is the gate pulse to obtain the correct torque value.

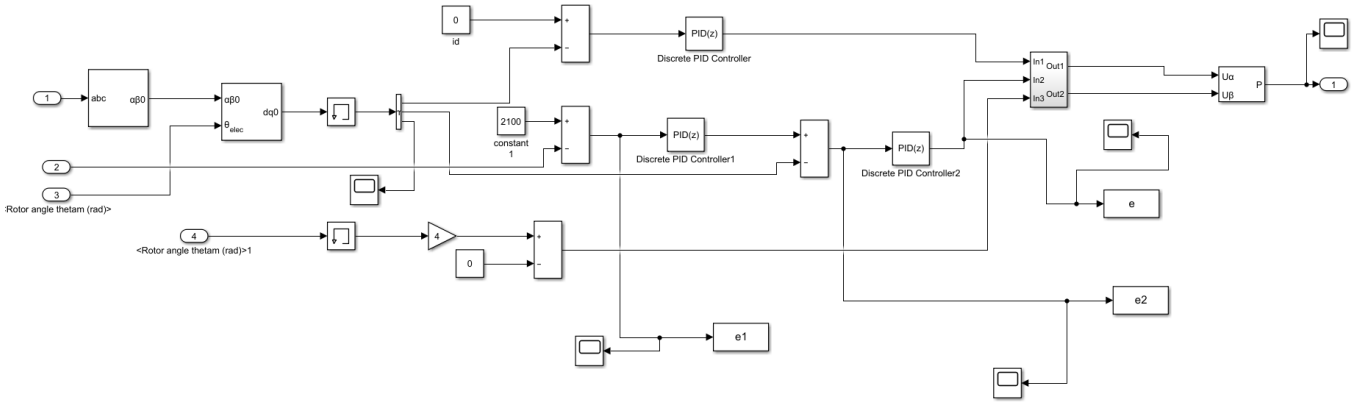

Figure 39- DTC-SVPWM SIMULINK model

Second system involved in the use of AIS mechanism is PID control that control the power value of the flywheel in the link with grid side.

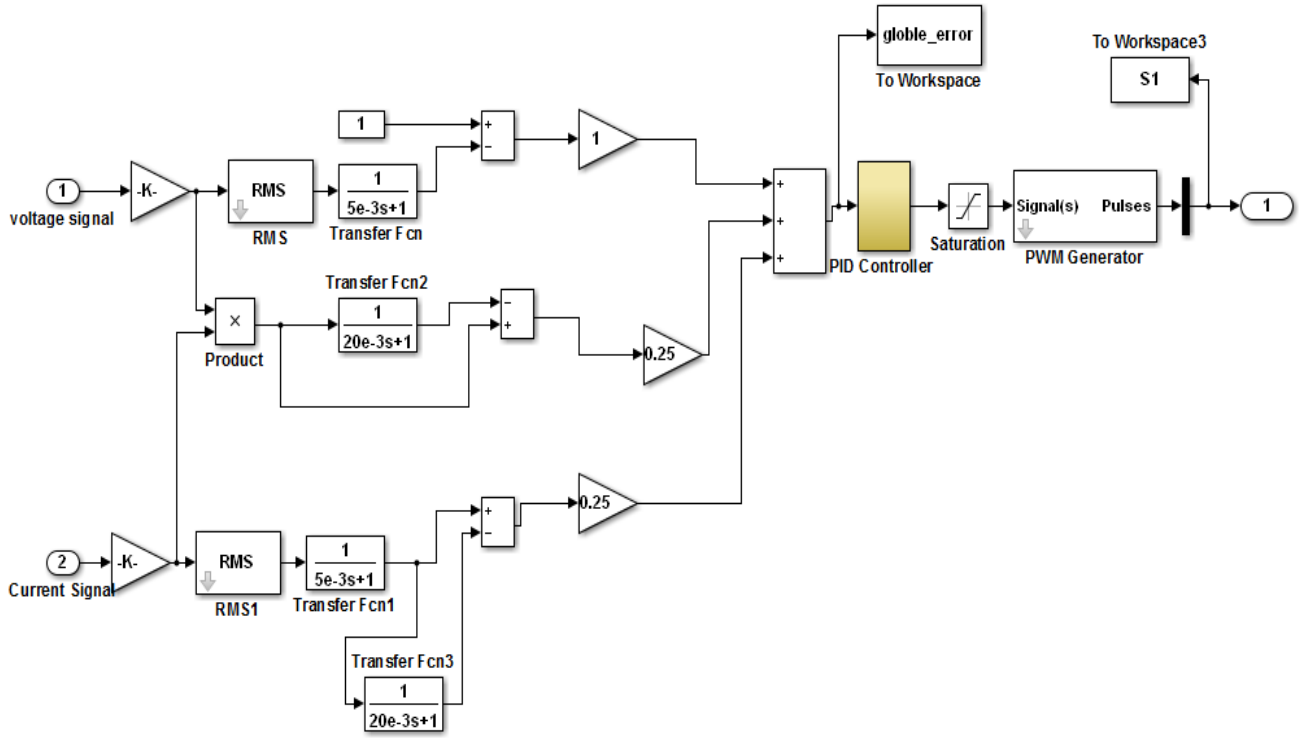

Figure 40- Power control system

SIMULINK model of flywheel component is designed in following figure. It is evident the presence of PMSM component and the blocks containing electromagnetic torque and energy storage system.

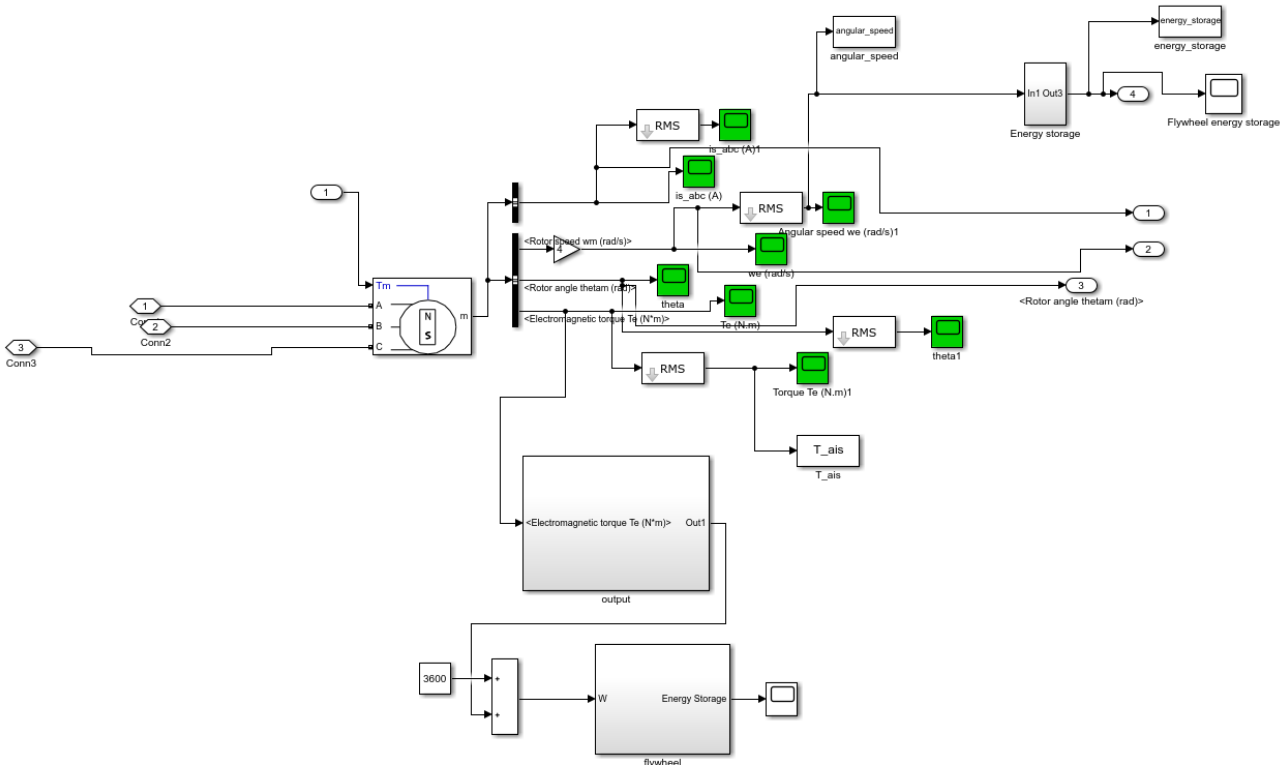

Figure 41-Flywheel SIMULINK model

Block parameters for permanent magnet synchronous machine are set in the general model and are represented in following figure:

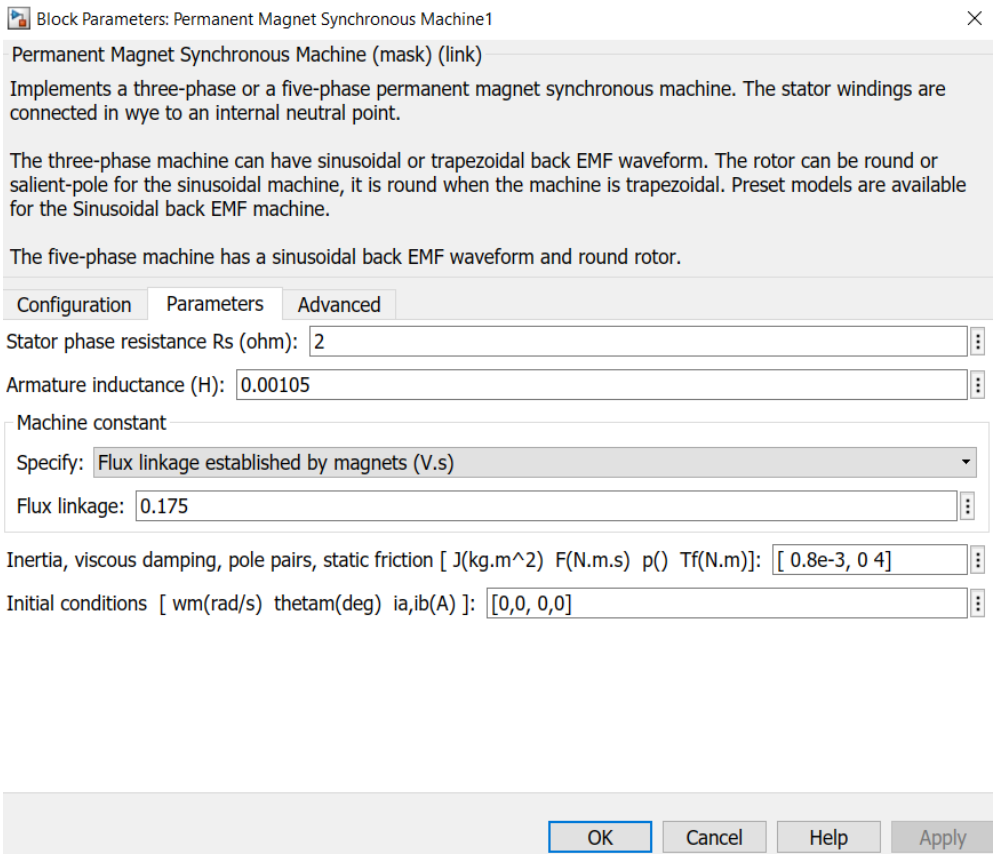

Figure 42- PMSM block parameters

Grid side is characterised by these parameters:

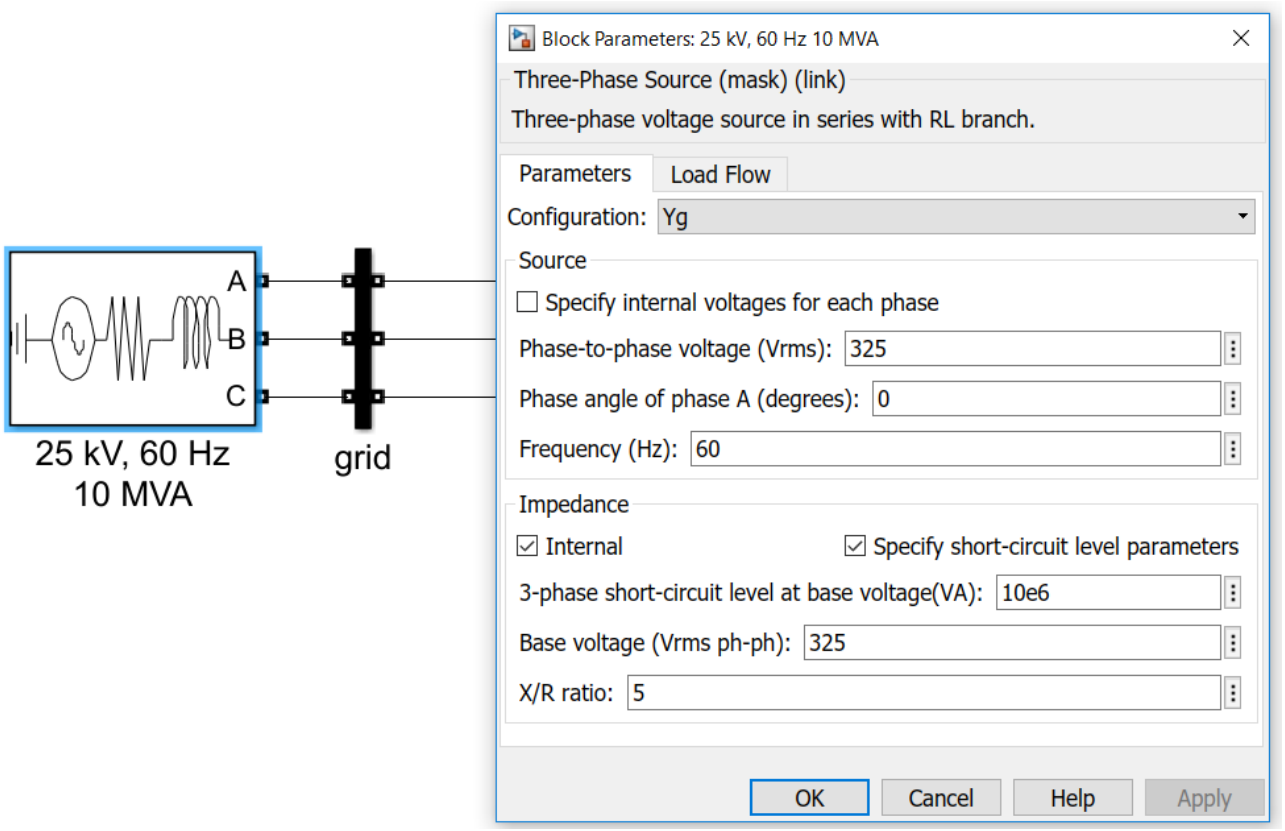

Figure 43- Grid block parameters

Another important component is the buttery system that simulate the presence of the bus under charging condition at the flywheel fast charging station.

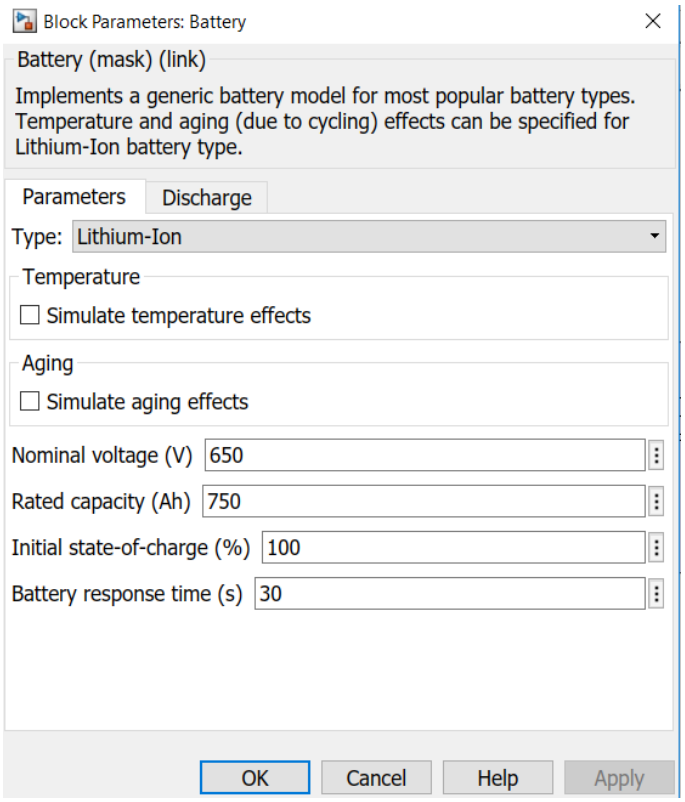

Figure 44- Battery block parameters

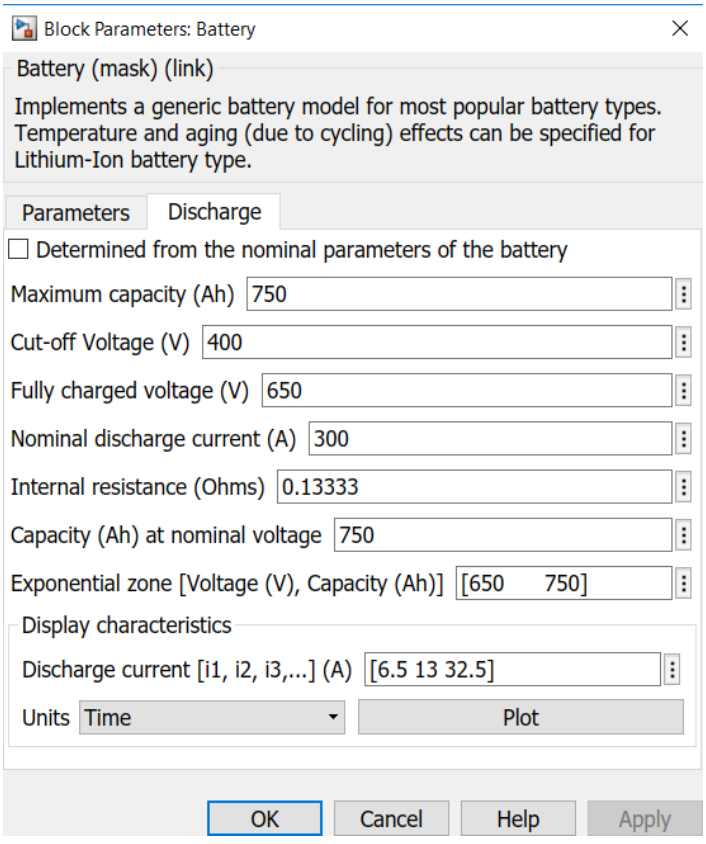

Figure 45- Battery discharge values

11) MATLAB IMPLEMENTATION

MATLAB/SIMULINK model is constructed in order to enhance the dynamic performance and increase the output parameters using SVPWM control, PID block will be controlled and tuned by minimizing the driven error signal with the application of an advanced computational intelligence technique [43][44], called Artificial Immune System (AIS).

Direct link with chapter of AIS algorithm is the definition of antibodies that are now represented by optimal solution of K_p, K_i, K_d values while antigens are the function that need to be optimized, represented in this case by the error involved in DTC and power system.

11.1) MATLAB CODE

Following figures show some basic tracks of CLONALG implementation for current work. Each step represents parallel passage of the AIS flowchart description.

First step is the selection of initial population and the evaluation of objective function. Some parameters can be changed by user and are contained in table previously described. MATLAB code runs into SIMULINK model through the called '***fit_fun***' function with following code:

```
sim('power_3levelVSC_version_2.slx',[0 0.1]);
```

Figure 46- Function to call SIMULINK model

```
%================================ ClonalG ================================
%-------------------------------------------------------------------------
% ClonalG
%-------------------------------------------------------------------------
for kImmune=1:KImmune_fin
%-------------------------------------------------------------------------

    minFw0 = fit_fun(w0,time,torque, angular_speed, energy_storage);
     if  minFw0 <= Max_error
         Sol=w0
         minFw0
         break
     end

%------------------------------ Selection ------------------------------
%-----------%
% Selection % %First selection of efficient Ab by order
%-----------%
for ksel=1:pop_size
    Sel_Ab_cri(ksel)=fit_fun(Ini_Ab(:,ksel)); % fitness estimation for all the select
end
% Order
Min_fit_sel=[];
Min_fit=[];
for ksel=1:pop_size

    [sel index]=min(Sel_Ab_cri);

    Min_fit=[Min_fit ,sel];
    Min_fit_sel=[ Min_fit_sel ,Ini_Ab(:,index) ]; % croissent order

    if index <= (length(Sel_Ab_cri))
        Sel_Ab_cri(index)=Sel_Ab_cri(end);
    end

    Sel_Ab_cri=Sel_Ab_cri(1:end-1);

end

Sel_best_pop=Min_fit_sel(:,1:best_pop_size); % Re-selection based on best selected po
Fit_best_pop=Min_fit(:,1:best_pop_size);

%--------------------------- *END* Selection ---------------------------
```

Figure 47- MATLAB code_1

After this first part there is the affinity assessment of the antibodies and the proportional proliferation of clones and successive somatic hypermutation.

Antibodies with best affinity measure will have greater number of clones.

```
% Clones % Best Ab clone
%---------%
Nc=[];
for kclone=1:best_pop_size

%-------------------------------- Maturate ---------------------------------
%----------%
% Maturate %
%----------%

%    maturat_rate=0.05*exp(-0.01*Fit_best_pop(kclone));% PID mliha (0.001,-0.01)
     maturat_rate=(Fit_best_pop(kclone)/50)*exp(-0.01*Fit_best_pop(kclone));% PID mli

    %clone_best_pop= Sel_best_pop(:,kclone)+ maturat_rate * (rand(Nbre_var,1)-rand(Nb
    %clone_best_pop= Sel_best_pop(:,kclone)+ maturat_rate * (rand(Nbre_var,1)-rand(Nb
     clone_best_pop= Sel_best_pop(:,kclone)+ maturat_rate * 1 *(rand(Nbre_var,1)-rand

%----------------------------- *END* Maturate ------------------------------
```

Figure 48- MATLAB code_2

```
       Nci_size=round((clone_size_factor*pop_size)/kclone); % Clone population size estim

       Nci=[];

       for kNci=1:Nci_size
           Nci=[Nci clone_best_pop];
       end

       Nc=[Nc Nci];    % Total clone

   end

   %------------------------------ *END* Clones -----------------------------
```

Figure 49- MATLAB code_3

New population now borne thanks to a perfect mix of best old parents and best member of population of clones.

```
%------------------------------ Re-Selection -----------------------------
%--------------%
% Re-Selection % %Re-selection of efficient Ab by re-order
%--------------%
[Nclin Nccol]=size(Nc);
for kNcsel=1:Nccol
    Sel_Nc_cri(kNcsel)=fit_fun(Nc(:,kNcsel));
end
% Order
Min_fit_Ncsel=[];

for kNcsel=1:length(Nc)

    [Ncsel index]=min(Sel_Nc_cri);

    %Min_fit=[Min_fit ,sel];
    Min_fit_Ncsel=[ Min_fit_Ncsel ,Nc(:,index) ];

    if index <= (length(Sel_Ab_cri))
        Sel_Nc_cri(index)=Sel_Nc_cri(end);
    end

    Sel_Nc_cri=Sel_Nc_cri(1:end-1);

end
```



```
Re_Sel_best_pop=[Min_fit_Ncsel(:,1:best_pop_size-1) Sol_tr];
%Re_Sel_best_pop=Min_fit_Ncsel(:,1:best_pop_size-1);

%--------------------------- *END* Re-Selection --------------------------
```

Figure 50- MATLAB code_4

Last step before the end of the cycle is the check of the stop criteria. If minimum threshold is lower than minimum error imposed at the beginning of the cycle or the maximum number of iterations is reached the work ends. If otherwise another cycle will run the population is updated with the fresh one just calculated.

```
%--------------------------------- Out Test ---------------------------------
%----------%
% Out Test %
%----------%

minFtr = fit_fun(Min_fit_Ncsel(:,1));
minF = fit_fun(Sol_tr);

    if minFtr <= minF

        Sol_tr = Min_fit_Ncsel(:,1);
        minF = minFtr;

    end

    minF;
    Sol_tr;

    minF_evolution = [minF_evolution minF];
%------------------------------%
% Best_Fitnes Convergence Plot %
%------------------------------%

%     if (nargin > 8)&(eva_plot == 'on')
%         kImmune_evolution = 0:1:(kImmune-1);
%         figure(1)
%         semilogy(kImmune_evolution, minF_evolution)
%         xlabel('Iteration Nbr')
%         ylabel( 'Best Fitness')
%         hold on
%     end
 pause (0.2)
    if  minF <= Max_error
        Sol=Sol_tr;
        break
    else

    Ini_Ab(:,1:best_pop_size)=Re_Sel_best_pop;
    %Ini_Ab(:,1:best_pop_size)=[w0 Re_Sel_best_pop];
    end
%------------------------------ *END* Out Test ------------------------------
```

Figure 51- MATLAB code_5

12) SIMULATION RESULTS AND WORK SCENARIO

12.1) OPTIMIZED PARAMETER

SIMULINK model is performed with the application of both AIS algorithm and GA to optimize the work of PID control inside DTC-SVPWM system.

The selected case studies are based on infrastructure for e-buses at downtown Toronto with simulated buses stops at distances of 3km, and with peak power 1.5MW and 10.06 kWh for the longest trip/stop.

Result of PID parameters coming from tuned AIS control are:

Controller	KP	KI	KD
PID	6.9	5.8	0.2

Table 8- PID optimized parameters

Following figure shows error trend during optimization work with the application of genetic algorithm (GA) and artificial immune system (AIS) methods.

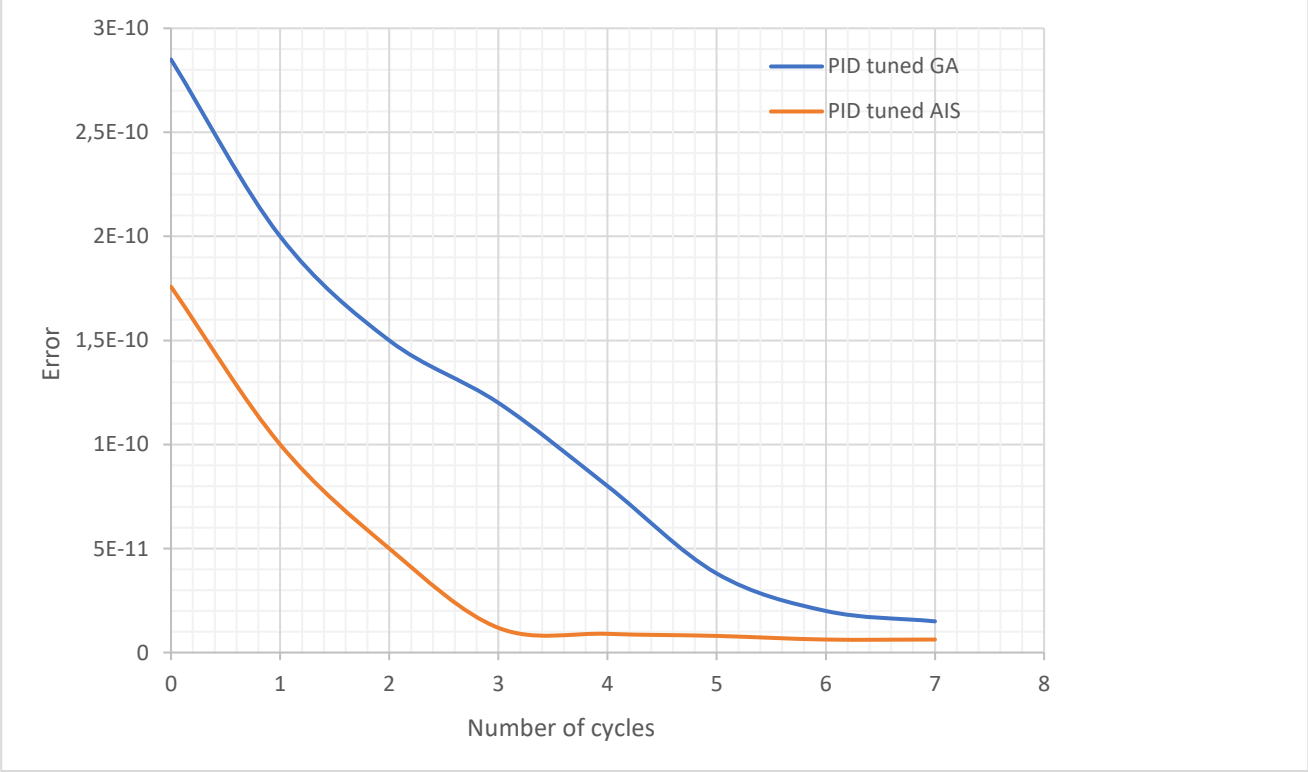

Figure 52- Error trend in two optimization processes

DTC enhance its performance due to the AIS PID control in the SVPWM mechanism. In the figure there is the trend of torque value in both cases, with traditional PID control and with tuned AIS application. In last case provided torque is higher than previous application and reach it stability in lower time than traditional work.

It is clear that the responses for the system with the proposed PID-EAIS control algorithms are outperforming other traditional technique; which confirms the effectiveness of the proposed FFCS control method.

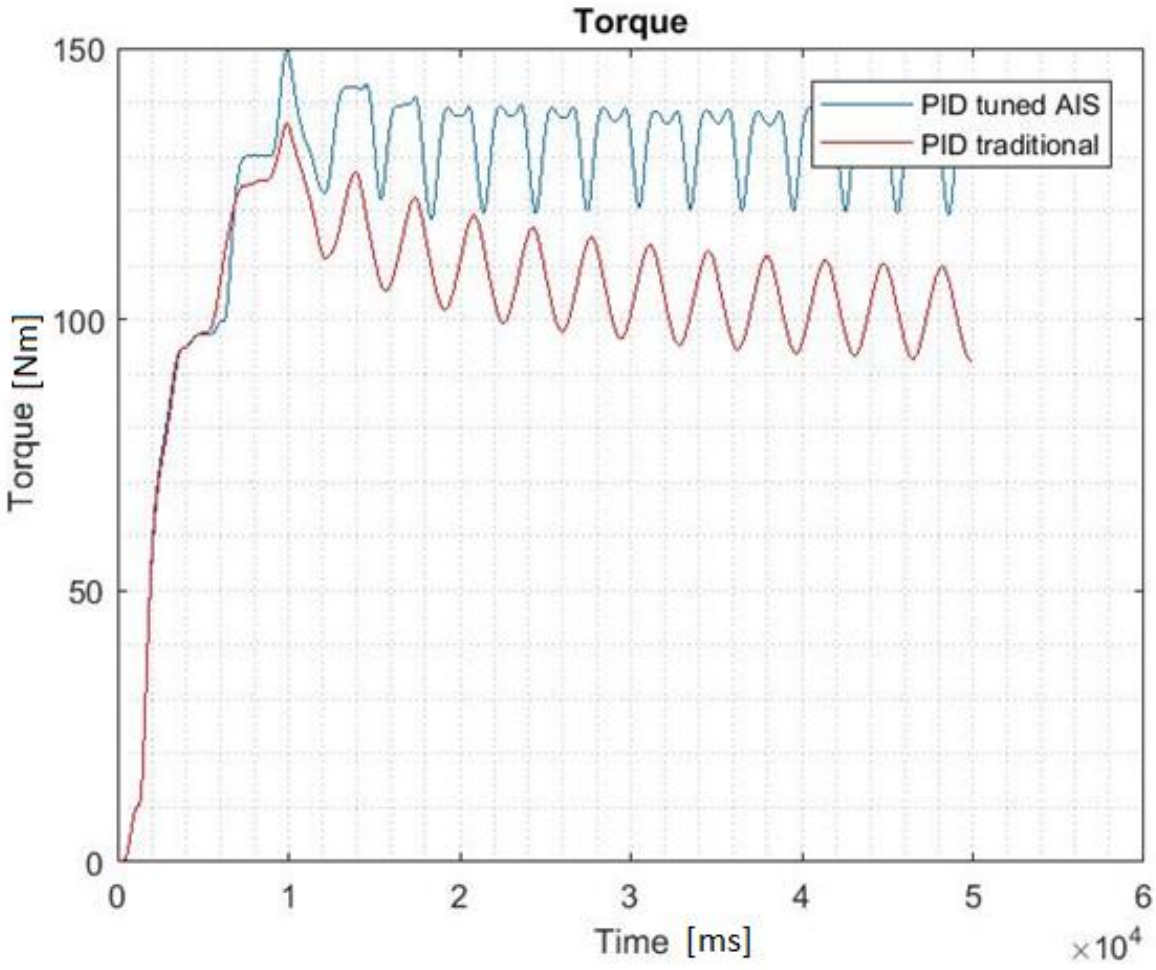

Figure 53- Torque enhancement during AIS application

The amount of energy that is outgoing from FFCS is higher when the proposed artificial immune system is applied as a control optimization method as integrated with PID control system. Simulation scenario

in table shows values for torque for the flywheel side during normal operation of charging cycles of the proposed FFCS fast charging station.

Parameters	Torque [Nm]	Time [ms]
with EAIS	130	$4.1 * 10^8$
without EAIS	95	$1.8 * 10^8$

Table 9- Value with and without AIS application

12.2) E-BUS WORK SIMULATION

Mechanical parameters involved in equations for ebus work are tabled. The simulation profile of the work of electric bus in Toronto is performed basing on actual values:

Variable	Description	Value
$N_{p,max}$	Maximum number of passengers	50 passengers
m_{RS}	Mass of rolling stock	34162 kg
v_{opp}	Operating speed	17m/s
$a_{acc,opp}$	Operating acceleration	$0.8 m/s^2$
$a_{dec,\,opp}$	Operating deceleration	$1.35 m/s^2$

Table 10- e-BUS mechanical parameters

Following figure 54 shows the simulation profile and energy/power data between two stations: St. Clair West to Eglinton West at downtown Toronto with the application of the proposed system. Table 7 shows the simulation results at different stations.

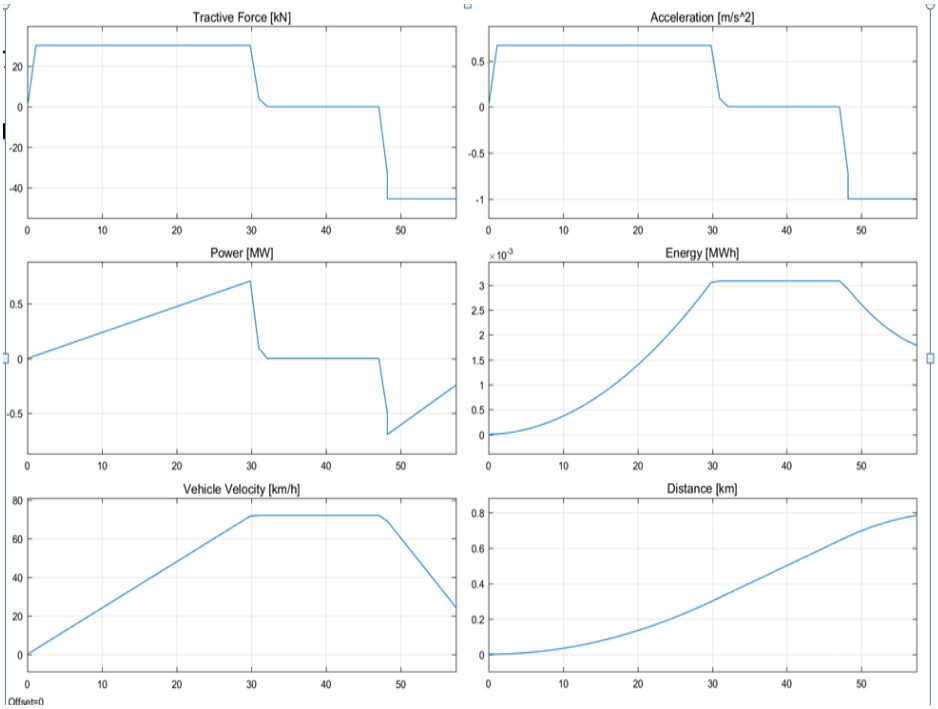

Figure 54- Trend of mechanical and electrical parameters during e-BUS work

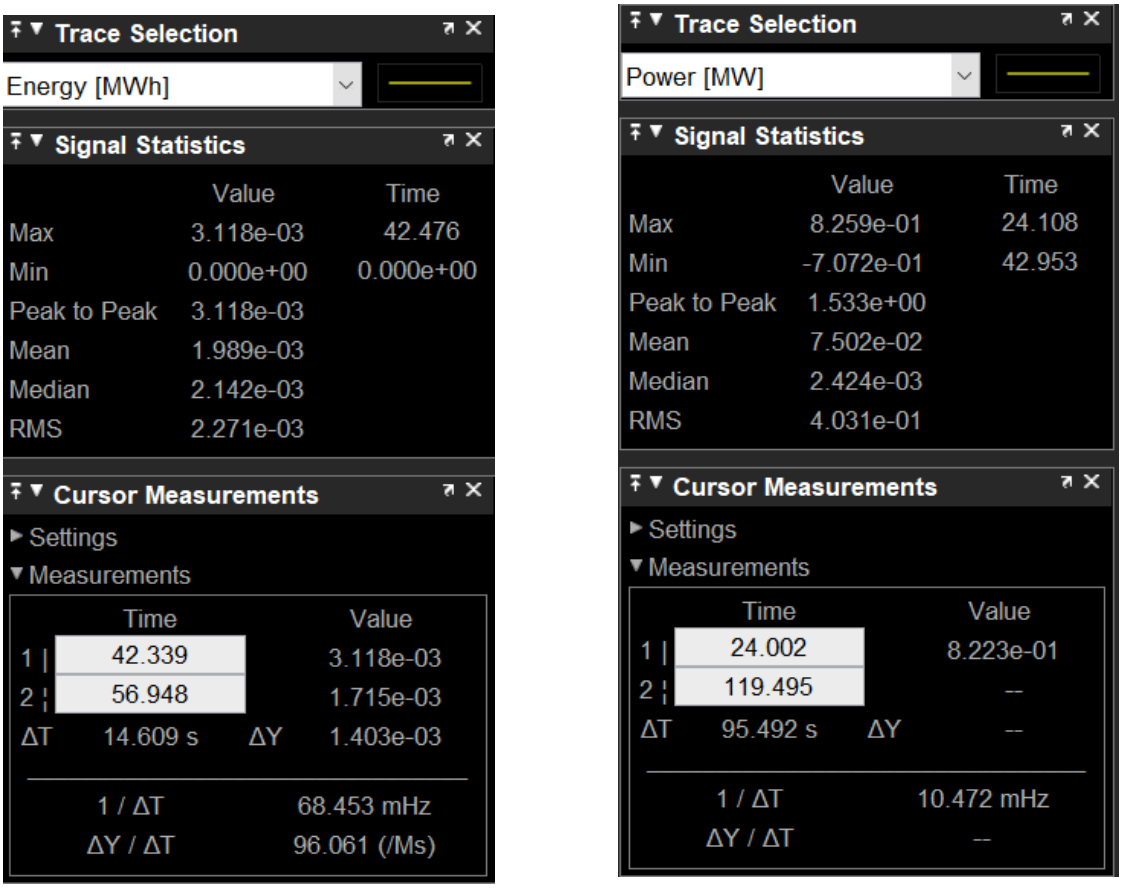

Figure 55- Energy and power values in St Clair West-Eglinton West track

	Queen's Park to Museum	Yonge to Bayview	St. Clair West to Eglinton West
Duration [s]	57.4	119.9	154.9
Distance [km]	0.750	2	2.7
Energy [kWh]	3.11	3.3	3.4
Peak Power [MW]	0.86	0.82	0.85

Table 11- Energy and power values in three different tracks

13) CONCLUSIONS

The work of this thesis was born from the idea to look forward to the future world of transport. This field is very wide, but the base concept is the switch from traditional to electric fuel to face larger consumption and pollution problems. In this context thesis focuses on e-bus public transportation and works on the optimization of two of the main tasks of this application: fast charging station placement and internal control of flywheel used as energy storage in the stations.

To perform this work various optimization algorithm and methods coming from artificial intelligence are applied with the use of MATLAB.

The optimal placement is a work that put out the best positions of the fast charging stations in the urban area in order to have the lower possible distance between each bus terminal and its relative charging station. This application lead to both less time and less power consumed to go to charge the battery.

First method involved in this application is descent gradient method that is a confirmed optimization algorithm to find the minimum of a function even with multivariable application.

Genetic algorithm is the second method applied in this work. It is a heuristic method of the field of artificial intelligence and is based on evolution theory of Darwin. Its application on MATLAB leads to another optimal solution for the placement of the stations in the urban area. Toronto is the case study for this application and the performance of future scenarios involves its public transportation network.

First result of this work is that initial positions of station points in the area influence final ones. In this way a combination of the two methods is performed after a starting individual performance and the final result is the better solution found after described applications.

Second half of the work focuses on the internal control of the energy storage system of the charging station. In particular actual studies design stations with flywheel as energy storage to have a better exploitation of renewable sources of energy even when they are not directly accessible. SIMULINK model of the station is performed and in particular optimization analysis works on the Direct Torque Control (DTC) of the flywheel. System with a higher value and a faster response performs with a PID control instead of a traditional hysteresis control. In addition the application of Artificial Immune System enhance the control performance. It is an artificial method from neural network that simulate the optimization process of the antibodies in a human body. In particular PID parameters are the principal of the process and their work leads to the progressive reduction of the involved error and then to optimized work. Final results is a higher torque value with a fast response to disturbance with respect to traditional application.

Both works face up to future electric bus network in the case study of Toronto. Optimization is obtained thanks to the application of special algorithms and neural network methods that try to simulate various natural processes in an artificial way.

Final conclusion is that the application of these methods is the correct way to reach more and more optimal solutions. Enhancement and deeper analysis of the algorithms will lead to better performance in future applications because this field has no conclusions but can be always improved.

14) REFERENCES

[1] Larry E. Erickson, Department of Chemical Engineering, Kansas State University, "Reducing Greenhouse Gas Emissions and Improving Air Quality: Two Global Challenges", Wiley Online Library, 2017.

[2] Preeti Aggarwal, Suresh Jain, "Impact of air pollutants from surface transport sources on human health: a modeling and epidemiological approach", Environment International (Elsevier), 2015.

[3] Sabine Wurzler, Heike Hebbinghaus, Ingo Steckelbach, Thomas Schulz, Wulf Pompetzki, Michael Memmesheimer, Hermann Jakobs, Tilmann Schöllnhammer, Sonja Nowag and Volker Diegmann, "Regional and local effects of electric vehicles on air quality and noise", Meteorologische Zeitschrift, Vol. 25, No. 3, 319–325, 2016.

[4] Perez L., Trüeb S., Cowie H., Keuken M.P., Mudu P., RagettliM.S., Sarigiannis D.A., Tobollik M., Tuomisto J., Vienneau D., Sabel C., Künzli N., "Transport-related measures to mitigate climate change in Basel, Switzerland: a health-effectiveness comparison study", Environment International (Elsevier), 2015.

[5] Helmers and Marx: "Electric cars: technical characteristics and environmental impacts.", Environmental Sciences Europe, 2012.

[6] Matthias Rogge, Sebastian Wollny, Dirk Uwe Sauer, "Fast Charging Battery Buses for the electrification of Urban Public Transport—A Feasibility Study Focusing on Charging Infrastructure and Energy Storage Requirements", Energies, 2015.

[7] Yu Huang1, Jingjing Ye2, Xin Du, Liyong Niu, "Simulation Study of System Operating Efficiency of EV Charging Stations with Different Power Supply Topologies", Trans Tech Publications, 2014.

[8] Michał Sierszyński, Michał Pikula, Paweł Fuć, Piotr Lijewski, Maciej Siedlecki, Marta Galant, "Overview of solutions for lithium-ion batteries used in electric vehicles", INTERNATIONAL JOURNAL OF ENERGY and ENVIRONMENT, 2016.

[9] Mohamed O. Badawy, Yilmaz Sozer, "Power Flow Management of a Grid Tied PV-Battery Powered Fast Electric Vehicle Charging Station", IEEE, 2015.

[10] WIREs Comput Stat 2014, 6:202–209. doi: 10.1002/wics.1298.

[11] Susanne Rothgang, Matthias Rogg, Jan Becker, Dirk Uwe Sauer, "Battery Design for Successful Electrification in Public Transport", Energies, 2015.

[12] N. Romero and R. B. Fernández, "Construction of Voronoi Diagram using

the Hollow Sphere Concept", IEEE, 2017.

[13] Dmitriy Morozov, Tom Peterka, "Efficient Delaunay Tessellation through K-D Tree Decomposition", IEEE, 2016.

[14] Chaoran Yang, S. W. Ricky Lee, "Investigation on the Thermal Degradation Mechanism of Cu-Sn Intermetallic Compound in SAC Solder Joints with Cohesive Zone Modeling", IEEE, 2015.

[15] Suman Debnath, Maryam Saeedifard," Simulation-Based Gradient-Descent Optimization of Modular Multilevel Converter Controller Parameters", IEEE, 2016.

[16] Bang Wang, Shengliang Zhou, Wenyu Liu, Yijun Mo, "Indoor Localization Based on Curve Fitting and Location Search Using Received Signal Strength", IEEE, 2015.

[17] Hsieh-chung chen, "Gradient descent for optimization problems with sparse solution", ProQuest LLC, 2017.

[18] Liying Song, Jun Wang, Dong Yang, "Optimal Placement of Electric Vehicle Charging Stations Based on Voronoi Diagram", IEEE, 2015.

[19] Piotr Faliszewski, Jakub Sawicki, Robert Schaefer, and Maciej Smołka, "Multiwinner voting in genetic algorithm", IEEE INTELLIGENT SYSTEMS, 2017.

[20] Abhishek Awasthi, Karthikeyan Venkitusamy, Sanjeevikumar Padmanaban, Rajasekar Selvamuthukumaran , Frede Blaabjerg , Asheesh K. Singh, "Optimal planning of electric vehicle charging station at the distribution system using hybrid optimization algorithm", Energy (Elsevier), 2017.

[21] Sidharth Iyer, D. Vijay Rao, "Genetic Algorithm based Optimization Technique for Underwater Sensor Network Positioning and Deployment", IEEE.

[22] G. Giftson Samuel, C. Christober Asir Rajan, "Hybrid: Particle Swarm Optimization–Genetic Algorithm and Particle Swarm Optimization–Shuffled Frog Leaping Algorithm for long-term generator maintenance scheduling", Electrical Power and Energy Systems (Elsevier), 2014.

[23] A. Arabali, M. Ghofrani, M. Etezadi-Amoli, M. S. Fadali, and Y. Baghzouz, "Genetic-Algorithm-Based Optimization Approach for Energy Management", IEEE, 2013.

[24] Pazos-Revilla, M., Alsharif, A., Gunukula, S., Nan, T.: 'Secure And Privacy-Preserving Physical-Layer-Assisted Scheme For EV Dynamic Charging System", IEEE Transactions on Vehicular Technology, 2017, 67, (4), pp 3304 - 3318

[25] Houlian, W., Gongbo, Z.: 'State of charge prediction of supercapacitors via combination of Kalman filtering and backpropagation neural network', IET Electric Power Applications, 2018, 12, (4), p. 588 - 594

[26] Sun, B., Dragicevic, T., Juan, C., Josep M.: 'Distributed Cooperative Control of Multi Flywheel Energy Storage System for Electrical Vehicle Fast Charging Stations', 17th European Conference on Power Electronics and Applications (EPE'15 ECCE-Europe), Geneva, 2015, pp 1-8

[27] Zine, W., et al.: 'Optimisation of HF signal injection parameters for EV applications based on sensorless IPMSM drives', Electric Power Applications, 2018, 12, (3), p. 635 – 641

[28] Yilmaz, M., Krein, P.: 'Review of battery charger topologies charging power levels and infrastructure for plug-in electric and hybrid vehicles', IEEE Trans. on Power Electron, 2013, 28, (5), pp. 2151-2169

[29] Wencong, S., Tao, J., Shaohui, W.: 'Modeling and Simulation of Short-term Energy Storage: Flywheel", International Conference on Advances in Energy Engineering ICAEE, 2010, China, pp. 1-8.

[30] Sun, B., Dragičević, T., Francisco, D., Juan C.: 'A Control Algorithm for Electric Vehicle Fast Charging Stations Equipped With Flywheel Energy Storage Systems', IEEE Transactions on Power Electronics, 2016, 31, (9), pp. 6674 – 6685

[31] Prasanna Sagdeo, Shilpa Patil, Vipinkumar Meshram , Puja Zurale, 'SVPWM controller for three phase inverter using PI controller operating under non linear load' , International Journal of Advanced Research in Computer and Communication Engineering, 2015.

[32] Vinoth Kumar, Prawin Angel Michael, Joseph P. John and Dr. S. Suresh Kumar, 'SIMULATION AND COMPARISON OF SPWM AND SVPWM CONTROL FOR THREE PHASE INVERTER K.', ARPN Journal of Engineering and Applied Sciences, 2010.

[33] Suraj Karpe, Sanjay A.Deokar, Arati M.Dixit, 'Switching losses minimization by using direct torque control of induction motor', Journal of Electrical Systems and Information Technology, 2017.

[34] S.L.Kaila, H.B.jani, 'Direct Torque Control for Induction Motor Using SVPWM Technique', National Conference on Recent Trends in Engineering & Technology, 2011.

[35] Hongxia Yu, Zhicheng Chen, 'Three-Phase Induction Motor DTC-SVPWM Scheme with Self-tuning PI-Type Fuzzy Controller, International Journal of Computer and Communication Engineering, 2015.

[36] Fauziah, S., Amir, T., Abdul Rahim, F., Mansor, H., and Akmeliawat, R.: 'PID tuned Artificial Immune System Hover Control for Lab-Scaled Helicopter System', IEEE, Control Conference (ASCC), Kota Kinabalu, Malaysia, June 2015, pp.1-6.

[37] De Castro Leandro N., Von Zuben Fernando J., Learning and optimization using the Clonal Selection principle.

[38] Repetto Maurizio, Stochastic optimization.

[39] Alonso, F., Oliveira, D., Zambroni A.: 'Artificial Immune Systems Optimization Approach for Multiobjective Distribution System Reconfiguration', IEEE Transactions on Power Systems, 2015, 30, (2), pp 840-847.

[40] Tousif Khan Nizami, K. Sundareswaran, "A Feedback Control Design of Buck Converter: An Artificial Immune System Based Approach".

[41] Sundareswaran, K., Devi., Nitin A. and Shrivastava, N.: 'Design and Development of a Feedback Controller for Boost Converter Using Artificial Immune System', Electric Power Components and Systems, 2011, 39, (10), pp. 1007-1018.

[42] Daoud, M. I., et al.: 'An artificial neural network-based power control strategy of low-speed induction machine flywheel energy storage system', Journal of Advances in Information Technology, 2013, 4, (2), pp. 61-68

[43] Grzegorz, D., Czestochowa, A.: 'Artificial Immune System With Local Feature Selection for Short-Term Load Forecasting', IEEE Transactions on Evolutionary Computation, 2017, 21, (1), pp 116-130.

[44] Fernando, P., Anna, P., Carlos R.: 'Wavelet-artificial immune system algorithm applied to voltage disturbance diagnosis in electrical distribution systems', IET Generation, Transmission & Distribution, 2015, 9, (11), pp 1101-1111.